Supporting Information

New Amidated 3,6-diphenylated Imidazopyridazines with Potent Antiplasmodium Activity are Dual Inhibitors of *Plasmodium* phosphatidylinositol-4-kinase and cGMP-dependent protein kinase

Peter Mubanga Cheuka,[†,‡] Luyanda Centani,[†] Lauren B. Arendse,[Ω,Π] Stephen Fienberg,[†,Π] Lynn Wambua,[†] Shoneeze S. Renga,[†] Godwin Akpeko Dziwornu,[†] Malkeet Kumar,[†] Nina Lawrence,[∞] Dale Taylor,[∞] Sergio Wittlin,[‖,⊥] Dina Coertzen,[§] Janette Reader,[§] Mariette van der Watt,[§] Lyn-Marie Birkholtz[§] and Kelly Chibale*[,†,Ω,Π]

[†]Department of Chemistry, University of Cape Town, Rondebosch 7701, Cape Town, South Africa.

[‡]Department of Chemistry, University of Zambia, Great East Road Campus, P.O Box 32379, Lusaka, Zambia.

[∞]Drug Discovery and Development Centre (H3D), Division of Clinical Pharmacology, Department of Medicine, University of Cape Town, Observatory 7925, Cape Town, South Africa.

[‖]Swiss Tropical and Public Health Institute, Socinstrasse 57, 4002 Basel, Switzerland.

[⊥]University of Basel, 4003 Basel, Switzerland.

[§]Department of Biochemistry, Genetics and Microbiology, Institute for Sustainable Malaria Control, University of Pretoria, Hatfield, Pretoria 0028, South Africa.

[Ω]Institute of Infectious Disease and Molecular Medicine, University of Cape Town, Rondebosch 7701, Cape Town, South Africa.

[Π]Drug Discovery and Development Centre (H3D) and South African Medical Research Council Drug Discovery and Development Research Unit, University of Cape Town, Rondebosch 7701, Cape Town, South Africa.

Corresponding author: *(K.C.) E-mail: kelly.chibale@uct.ac.za

Table of Contents

1.0 Synthetic Procedures and/or Characterization Data for Other Compounds S3
2.0 Biological and Solubility Evaluation S12
3.0 Supplementary Tables S1, S2 and S3 .....S20
4.0 ^{1}H-NMR Spectra of Selected Compounds S24
5.0 Additional References.....S30

1.0 Synthetic Procedures and/or Characterization Data for Other Compounds

*(4-(6-(3-(Methylsulfinyl)phenyl)imidazo[1,2-b]pyridazin-3-yl)phenyl)(piperazin-1-yl)methanone (**6**).* To the solution of the boc-protected intermediate **6i** (0.0181 g, 0.033 mmol) in DCM (2 mL) cooled in an ice bath was added trifluoroacetic acid (0.2 mL, 2.6 mmol) dropwise over 30 min. The reaction mixture was left to stir at room temperature for 90 min (Note: The reaction generates gaseous products and was, therefore, left to take place under open atmosphere). Trifluoroacetic acid and DCM were removed *in vacuo* where after the resulting residue was taken up in 10% CH_3OH/DCM and neutralized using Amberlyst A21 for 90 min. After removing the solvent *in vacuo*, the obtained residue was purified by prep-TLC (developed in 10% CH_3OH/DCM). Yellow solid (0.015 g, 98%); R_f (CH_3OH : CH_2Cl_2 5 : 95) = 0.14; ^{1}H NMR δ_H (400 MHz, DMSO-d_6) 8.99 (s, 1H), 8.43 (d, J = 9.7 Hz, 1H), 8.41 (s, 1H), 8.38 (d, J = 8.5 Hz, 2H), 8.31 (d, J = 8.0 Hz, 1H), 8.02 (d, J = 9.6 Hz, 1H), 7.89 (d, J = 8.0 Hz, 1H), 7.82 (t, J = 7.7 Hz, 1H), 7.67 (d, J = 8.5 Hz, 2H), 4.22 (s, 1H), 3.76 (m, 4H), 3.52 (m, 4H), 2.86 (s, 3H); ^{13}C-NMR δ_C (151 MHz, Methanol-d_4) 172.0, 152.3, 147.6, 141.1, 138.2, 136.2, 134.3, 131.5, 131.3, 131.0, 129.3, 128.7 (2C), 127.9 (2C), 127.1, 126.5, 123.4, 117.9, 49.9, 46.8, 46.3, 44.2, 43.7; LC-MS, APCI$^+$: *m/z* $[M + H]^+$ = 446.1, calculated exact mass = 445.1572, purity = 98%, t_r = 2.65 min.

*4-(6-(3-(Methylsulfonyl)phenyl)imidazo[1,2-b]pyridazin-3-yl)benzoic acid (**7a**).* Yellow solid (0.798 g, 41%); R_f (CH_3OH : CH_2Cl_2 4 : 96) = 0.38; ^{1}H-NMR δ_H (400 MHz, DMSO-d_6) 8.67 (t, J = 1.76 Hz, 1H), 8.52 (dt, J = 7.92, 1.91 Hz, 1H), 8.43 (s, 1H), 8.40 (d, J = 9.51 Hz, 1H), 8.34 (d, J = 8.70 Hz, 2H), 8.12 (dt, J = 7.84, 1.85 Hz, 1H), 8.09 (d, J = 8.31 Hz, 2H), 8.05 (d, J = 9.55 Hz, 1H), 7.91 (t, J = 7.85 Hz, 1H), 3.35 (s, 3H); ^{13}C-NMR δ_C (101 MHz, DMSO-d_6) 168.44, 150.23, 142.44, 140.08, 136.79, 135.04, 132.36, 131.21, 130.96 (2C), 130.06 (2C), 128.82, 127.78, 127.17, 126.09 (2C), 125.87, 116.57, 43.96; LC-MS, APCI$^+$: *m/z* $[M + H]^+$ = 393.8, calculated exact mass = 393.0783, Purity = 97%, t_r = 3.56 min.

*(4-(6-(3-(Methylsulfinyl)phenyl)imidazo[1,2-b]pyridazin-3-yl)phenyl)(morpholino)methanone (**7**).* Purified by prep-TLC (developed in 2% CH_3OH/DCM, then 3% CH_3OH/DCM). Yellow solid (0.0653 g, 46.6%); m.p = 248.3 – 250.3 °C; R_f (CH_3OH : CH_2Cl_2 5 : 95) = 0.43; ^{1}H-NMR δ_H (400 MHz, $CDCl_3$) 8.48 – 8.33 (br s, 1H), 8.35 (s, 1H), 8.23 – 8.17 (m, 4H), 7.86 – 7.71 (m, 3H), 7.64 (d, *J* = 8.17 Hz, 2H), 3.88 – 3.58 (m, 8H), 2.84 (s, 3H); ^{13}C-NMR δ_C (101 MHz, $CDCl_3$) 169.95, 150.87, 147.34, 136.99 (2C), 134.86, 130.23, 129.62, 127.79 (3C), 126.86 (2C), 126.74, 126.45, 125.15, 122.10 (2C), 116.10, 67.10 (2C), 66.93 (2C), 44.12; LC-MS, APCI$^+$: *m/z* $[M + H]^+$ = 447.1, calculated exact mass = 446.1413, purity = 99.9%, t_r = 3.48 min.

*(4-Hydroxypiperidin-1-yl)(4-(6-(3-(methylsulfinyl)phenyl)imidazo[1,2-b]pyridazin-3-yl)phenyl)methanone (**8**).* Purified by prep-TLC (developed in 4% CH_3OH/DCM). Yellow solid (0.0127 g, 9%); R_f (CH_3OH : CH_2Cl_2 5 : 95) = 0.41; ^{1}H-NMR δ_H (600 MHz, Methanol-d_4) 8.38 (t, *J* = 1.7 Hz, 1H), 8.28 – 8.24 (m, 2H), 8.22 (ddd, *J* = 7.8, 1.9, 1.1 Hz, 1H), 8.17 (s, 1H), 8.12 (d, *J* = 9.5 Hz, 1H), 7.83 (d, *J* = 9.5 Hz, 1H), 7.81 (ddd, *J* = 7.8, 1.8, 1.1 Hz, 1H), 7.73 (t, *J* = 7.8 Hz, 1H), 7.59 – 7.55 (m, 2H), 4.26 - 4.14 (m, 1H), 3.91 (tt, *J* = 8.2, 3.8 Hz, 1H), 3.74 (s, 1H), 3.43 – 3.27 (m, 2H), 2.86 (s, 3H), 2.06 - 1.74 (m, 2H), 1.66 - 1.45 (m, 2H); ^{13}C-NMR δ_C (151 MHz, Methanol-d_4) 172.0, 152.3, 147.6, 141.1, 138.1, 136.5, 134.2, 131.5, 131.2, 131.0, 129.3, 128.4 (2C), 127.9 (2C), 127.0, 126.5, 123.4, 117.9, 67.7, 44.4, 43.7, 38.0, 35.6, 34.2; LC-MS, APCI$^+$: *m/z* $[M + H]^+$ = 461.1, calculated exact mass = 460.1569, purity = 99.9%, t_r = 3.39 min.

*(3-Hydroxypyrrolidin-1-yl)(4-(6-(3-(methylsulfinyl)phenyl)imidazo[1,2-b]pyridazin-3-yl)phenyl)methanone (**9**).* Purified by prep-TLC (developed in 2% CH_3OH/DCM, then 4% CH_3OH/DCM). Yellow solid (0.028 g, 20%); R_f (CH_3OH : CH_2Cl_2 5 : 95) = 0.55; ^{1}H-NMR δ_H (300 MHz, Methanol-d_4) 8.49 (t, *J* = 1.10 Hz, 1H), 8.41 – 8.31 (m, 3H), 8.30 – 8.21 (m, 2H), 7.96 (d, *J* = 9.40 Hz, 1H), 7.89 (dt, *J* = 7.49, 1.88 Hz, 1H), 7.84 (t, *J* = 8.49 Hz, 1H), 7.76 (d, *J* = 7.76 Hz, 2H), 4.57 – 4.50 (m, 1H), 4.46 – 4.39 (m, 1H), 3.89 – 3.71 (m, 3H), 2.91 (s, 3H),

2.23 – 1.87 (m, 3H); ^{13}C-NMR δ_C (101 MHz, $CDCl_3$) 169.57, 150.58, 150.39, 147.14, 147.04, 137.05, 136.28, 136.06, 133.85, 133.62, 130.16, 129.61, 129.50 (2C), 127.74 (2C), 126.46, 125.06, 122.04, 115.70, 53.40, 44.07, 29.68, 22.67; LC-MS, APCI$^+$: *m/z* $[M + H]^+$ = 447.1, calculated exact mass = 446.1413, purity = 99.9%, t_r = 3.27 min.

*(3-Hydroxyazetidin-1-yl)(4-(6-(3-(methylsulfinyl)phenyl)imidazo[1,2-b]pyridazin-3-yl)phenyl)methanone (**10**).* Purified by prep-TLC (developed in 2% CH_3OH/DCM, then 5% CH_3OH/DCM). Yellow solid (0.0249 g, 13.4%); R_f (CH_3OH : CH_2Cl_2 5 : 95) = 0.21; ^{1}H-NMR δ_H (400 MHz, $CDCl_3$) 8.32 – 8.30 (br s, 1H), 8.20 (d, *J* = 8.48 Hz, 2H), 8.17 – 8.11 (m, 3H), 7.79 (d, *J* = 8.46 Hz, 2H), 7.75 – 7.69 (m, 2H), 7.65 (d, *J* = 9.45 Hz, 1H), 4.82 – 4.71 (m, 1H), 4.64 – 4.47 (m, 2H), 4.23 (m, 2H), 2.83 (s, 3H); ^{13}C-NMR δ_C (101 MHz, $CDCl_3$) 169.79, 150.53, 147.08, 137.06, 134.19, 132.37, 131.09 (2C), 130.23, 129.61, 128.41 (2C), 126.49 (2C), 126.39, 125.07, 122.06 (3C), 115.70, 61.97, 44.05, 29.68; LC-MS, APCI$^+$: *m/z* $[M + H]^+$ = 433.1, calculated exact mass = 432.1256, purity = 96%, t_r = 3.29 min.

*N-Methyl-4-(6-(3-(methylsulfinyl)phenyl)imidazo[1,2-b]pyridazin-3-yl)benzamide (**11**).* Purified by column chromatography (silica, 0 - 4% CH_3OH/DCM) followed by trituration in diethyl ether. Yellow solid (0.0329 g, 28%); R_f (CH_3OH : CH_2Cl_2 4 : 96) = 0.23; ^{1}H-NMR δ_H (300 MHz, DMSO-d_6) 8.53 (q, *J* = 4.60 Hz, 1H), 8.48 (s, 1H), 8.43 (t, *J* = 1.87 Hz, 1H), 8.38 (d, *J* = 10.09 Hz, 2H), 8.32 (dt, *J* = 7.56, 1.16 Hz, 1H), 8.09 – 7.98 (m, 4H), 7.90 (dt, *J* = 7.75, 1.51 Hz, 1H), 7.83 (t, *J* = 7.66 Hz, 1H), 2.87 (s, 3H), 2.83 (d, *J* = 4.47 Hz, 3H); LC-MS, APCI$^+$: *m/z* $[M + H]^+$ = 391.1, calculated exact mass = 390.1150, purity = 97%, t_r = 3.50 min.

*N,N-Dimethyl-4-(6-(3-(methylsulfinyl)phenyl)imidazo[1,2-b]pyridazin-3-yl)benzamide (**12**).* Purified by prep-TLC (developed twice in 3% CH_3OH/DCM). Yellow oil (0.0285 g, 24%); R_f (CH_3OH : CH_2Cl_2 5 : 95) = 0.69; ^{1}H-NMR δ_H (300 MHz, DMSO-d_6) 8.43 – 8.41 (m, 2H), 8.38 – 8.30 (m, 4H), 8.00 (d, *J* = 9.54 Hz, 1H), 7.89 (dt, *J* = 7.73, 2.35 Hz, 1H), 7.82 (t, *J* = 7.68 Hz, 1H), 7.60 (d, *J* = 8.20 Hz, 2H), 3.06 – 2.97 (br s, 6H), 2.86 (s, 3H); ^{13}C-NMR δ_C (101 MHz, $CDCl_3$) 171.17, 150.46, 147.25, 137.15, 135.79 (2C), 130.21, 129.62 (3C), 127.68

(3C), 126.64, 125.01, 122.05 (3C), 115.61, 44.15, 29.68 (2C); LC-MS, APCI$^+$: *m/z* $[M + H]^+$ = 405.1, calculated exact mass = 404.1307, purity = 98%, t_r = 3.60 min.

N-Allyl-4-(6-(3-(methylsulfinyl)phenyl)imidazo[1,2-b]pyridazin-3-yl)benzamide ***(13)***. Purified by prep-TLC (developed twice in 2% CH_3OH/DCM). Yellow solid (0.0232 g, 14%); R_f (CH_3OH : CH_2Cl_2 2 : 98) = 0.32; ^{1}H-NMR δ_H (600 MHz, Methanol-d_4) 8.41 (t, *J* = 1.8 Hz, 1H), 8.29 – 8.25 (m, 2H), 8.24 – 8.21 (m, 1H), 8.18 (s, 1H), 8.13 (d, *J* = 9.5 Hz, 1H), 7.98 (d, *J* = 8.5 Hz, 2H), 7.86 – 7.81 (m, 2H), 7.75 (t, *J* = 7.57 Hz, 1H), 6.00 (ddt, *J* = 17.1, 10.3, 5.5 Hz, 1H), 5.30 (dq, *J* = 17.1, 1.7 Hz, 1H), 5.18 (dq, *J* = 10.3, 1.5 Hz, 1H), 3.36 – 3.28 (m, 2H), 2.89 (s, 3H); ^{13}C-NMR δ_C (151 MHz, Methanol-d_4) 167.97, 150.86, 146.36, 139.85, 136.81, 134.26, 133.54, 133.10, 131.25, 130.02, 129.53, 127.94, 127.34 (2C), 126.17 (2C), 125.64, 125.11, 121.99, 116.34, 114.98, 42.34, 41.98; LC-MS, APCI$^+$: *m/z* $[M + H]^+$ = 416.8, calculated exact mass = 416.1307, purity = 97%, t_r = 2.66 min.

N-(2-Methoxyethyl)-4-(6-(3-(methylsulfinyl)phenyl)imidazo[1,2-b]pyridazin-3-yl)benzamide ***(14)***. Purified by prep-TLC (developed in 2% CH_3OH/DCM). Yellow solid (0.158 g, 69%); R_f (CH_3OH : CH_2Cl_2 2 : 98) = 0.40; ^{1}H-NMR δ_H (300 MHz, Methanol-d_4) 8.45 (t, *J* = 1.8 Hz, 1H), 8.35 – 8.25 (m, 3H), 8.24 (s, 1H), 8.18 (d, *J* = 9.6 Hz, 1H), 7.99 (d, *J* = 9.37 Hz, 2H), 7.94 – 7.81 (m, 2H), 7.79 (t, *J* = 7.7 Hz, 1H), 3.63 (s, 4H), 3.43 (s, 3H), 2.91 (s, 3H); ^{13}C-NMR δ_C (101 MHz, Methanol-d_4) 168.19, 150.70, 146.16, 136.61, 133.33, 133.06, 131.16, 130.04, 129.48, 127.33 (2C), 125.99 (2C), 125.57 (2C), 125.12 (2C), 121.91, 116.32, 70.66, 57.60, 42.30, 39.42; LC-MS, APCI$^+$: *m/z* $[M + H]^+$ = 434.8, calculated exact mass = 434.1413, purity = 98%, t_r = 3.01 min.

N-(2-Hydroxyethyl)-4-(6-(3-(methylsulfinyl)phenyl)imidazo[1,2-b]pyridazin-3-yl)benzamide ***(15)***. Purified by prep-TLC (developed in 4% CH_3OH/DCM). Yellow solid (0.071 g, 10%); R_f (CH_3OH : CH_2Cl_2 10 : 90) = 0.48; ^{1}H-NMR δ_H (300 MHz, Methanol-d_4) 8.62 (t, *J* = 1.59 Hz, 1H), 8.58 – 8.51 (m, 2H), 8.44 (d, *J* = 9.64 Hz, 1H), 8.37 (dt, *J* = 7.84, 1.40 Hz, 1H), 8.31 (d, *J* = 8.45 Hz, 2H), 8.10 (d, *J* = 8.55 Hz, 2H), 7.94 (dt, *J* = 7.87, 1.48 Hz,

1H), 7.86 (t, J = 7.76 Hz, 1H), 3.78 (t, J = 5.79 Hz, 2H), 3.58 (t, J = 5.83 Hz, 2H), 2.92 (s, 3H); ^{13}C-NMR δ_C (151 MHz, DMSO-d_6) 166.26, 151.58, 148.21, 139.41, 136.33, 134.18, 132.77, 130.77, 130.72, 129.74, 128.18, 127.71 (2C), 126.51 (2C), 125.99 (2C), 122.73, 118.20, 60.23, 43.70, 42.70; LC-MS, APCI$^+$: *m/z* $[M + H]^+$ = 421.1, calculated exact mass = 420.1256, purity = 95%, t_r = 2.08 min.

*N-(1-Hydroxybutan-2-yl)-4-(6-(3-(methylsulfinyl)phenyl)imidazo[1,2-b]pyridazin-3-yl)benzamide (**16**)*. Purified by prep-TLC (developed in 4% CH_3OH/DCM). Yellow solid (0.0273 g, 38%); R_f (CH_3OH : CH_2Cl_2 8 : 92) = 0.36; ^{1}H-NMR δ_H (400 MHz, DMSO-d_6) 8.44 (s, 1H), 8.42 (t, J = 1.8 Hz, 1H), 8.40 – 8.35 (m, 3H), 8.32 (dt, J = 7.7, 1.8 Hz, 1H), 8.19 – 8.02 (m, 3H), 8.00 (d, J = 9.6 Hz, 1H), 7.89 (dt, J = 8.20, 2.94 Hz, 1H), 7.83 (t, J = 7.8 Hz, 1H), 4.65 (t, J = 5.7 Hz, 1H), 3.97 – 3.85 (m, 1H), 3.52 (dt, J = 10.8, 5.4 Hz, 1H), 3.44 (dt, J = 11.0, 5.7 Hz, 1H), 2.87 (s, 3H), 1.78 – 1.63 (m, 1H), 1.57 – 1.42 (m, 1H), 0.92 (t, J = 7.4 Hz, 3H); ^{13}C-NMR δ_C (101 MHz, DMSO-d_6) 166.22, 150.96, 148.27, 140.14, 136.71, 135.03, 134.24, 131.26, 130.66, 129.62, 128.27 (2C), 127.48, 127.12, 126.12 (2C), 125.73, 122.70, 116.80, 63.61, 53.63, 43.76, 24.17, 11.12; LC-MS, APCI$^+$: *m/z* $[M + H]^+$ = 449.0, calculated exact mass = 448.1569, purity = 99.9%, t_r = 0.834 min.

*N-Cyclopropyl-4-(6-(3-(methylsulfinyl)phenyl)imidazo[1,2-b]pyridazin-3-yl)benzamide (**17**)*. Purified by prep-TLC (developed in 6% CH_3OH/DCM). Yellow solid (0.071 g, 43%); R_f (CH_3OH : CH_2Cl_2 10 : 90) = 0.59; ^{1}H-NMR δ_H (300 MHz, DMSO-d_6) 8.53 (d, J = 4.2 Hz, 1H), 8.45 (d, J = 0.8 Hz, 1H), 8.43 – 8.34 (m, 4H), 8.31 (d, J = 7.5 Hz, 1H), 8.05 – 7.96 (m, 3H), 7.89 (d, J = 7.7 Hz, 1H), 7.82 (t, J = 7.7 Hz, 1H), 2.87 (m, 4H), 0.73 (q, J = 6.3 Hz, 2H), 0.66 – 0.58 (m, 2H); ^{13}C-NMR δ_C (101 MHz, DMSO-d_6) 167.39, 150.93, 148.26, 140.14, 136.69, 135.04, 133.74, 131.35, 130.63, 129.62, 128.12 (2C), 127.42, 127.09, 126.12 (2C), 125.72, 122.67, 116.80, 43.77, 23.58, 6.22 (2C); LC-MS, APCI$^+$: *m/z* $[M + H]^+$ = 417.0, calculated exact mass = 416.1307, purity = 97%, t_r = 0.858 min.

*N-Methyl-4-(6-(3-(methylsulfonyl)phenyl)imidazo[1,2-b]pyridazin-3-yl)benzamide (**18**).* Purified by prep-TLC (developed in 3.5% CH_3OH/DCM). Yellow solid (0.0263 g, 17%); R_f (CH_3OH : CH_2Cl_2 10 : 90) = 0.73; ^{1}H-NMR δ_H (400 MHz, DMSO-d_6) 8.65 (t, J = 1.8 Hz, 1H), 8.50 (dt, J = 7.8, 1.9 Hz, 1H), 8.46 (s, 1H), 8.39 (m, 3H) 8.13 (dt, J = 7.8, 1.8 Hz, 1H), 8.03 (m, 3H), 7.90 (t, J = 7.9 Hz, 1H), 3.35 (s, 3H), 2.86 – 2.81 (m, 3H); ^{13}C-NMR δ_C (101 MHz, DMSO-d_6) 166.55, 150.37, 142.43, 136.83, 135.17, 133.88, 132.37, 131.25, 130.92, 128.83, 127.99, 127.46, 127.19, 126.24 (2C), 125.90, 116.73 (2C), 43.94, 40.50, 26.74; LC-MS, APCI$^+$: *m/z* $[M + H]^+$ = 406.8, calculated exact mass = 406.1100, purity = 99%, t_r = 3.33 min.

*N-(2-Methoxyethyl)-3-(3-(4-(methylsulfinyl)phenyl)imidazo[1,2-b]pyridazin-6yl)benzamide (**20**).* Purified by prep-TLC (developed in 0-10% CH_3OH/DCM with a few drops of 7 M aqueous ammonia). Yellow solid (0.049 g, 43%); R_f (CH_3OH : CH_2Cl_2 10 : 90) = 0.49; ^{1}H-NMR δ_H (600 MHz, DMSO-d_6) 8.74 (t, J = 5.15 Hz, 1H), 8.56 (t, J = 1.82 Hz, 1H), 8.48 (d, J = 8.53 Hz, 2H), 8.42 (s, 1H), 8.38 (d, J = 9.51 Hz, 1H), 8.30 (dt, J = 7.80, 1.90 Hz, 1H), 8.02 (dt, J = 7.79, 1.34 Hz, 1H), 7.99 (d, J = 9.57 Hz, 1H), 7.86 (d, J = 8.50 Hz, 2H), 7.69 (t, J = 7.8 Hz, 1H), 3.52 – 3.46 (m, 4H), 3.29 (s, 3H), 2.81 (s, 3H); ^{13}C-NMR δ_C (151 MHz, DMSO-d_6) 166.25, 151.38, 145.82, 140.14, 135.75, 135.63, 134.98, 131.13, 130.06, 129.80, 129.53 (2C), 127.18 (2C), 127.15, 127.07, 126.33, 124.63, 116.93, 71.01, 58.45, 43.64, 42.78; LC-MS, APCI$^+$: *m/z* $[M + H]^+$ = 435.1, calculated exact mass = 434.1413, purity = 97%, t_r = 2.93 min.

*N-Allyl-3-(3-(4-(methylsulfinyl)phenyl)imidazo[1,2-b]pyridazin-6-yl)benzamide (**22**).* Purified by prep-TLC (developed in 6% EtOH/DCM). Yellow solid (0.066 g, 60%); R_f (CH_3OH : CH_2Cl_2 10 : 90) = 0.49; ^{1}H-NMR δ_H (300 MHz, DMSO-d_6) 8.74 (t, J = 5.15 Hz, 1H), 8.56 (t, J = 1.82 Hz, 1H), 8.48 (d, J = 8.53 Hz, 2H), 8.42 (s, 1H), 8.38 (d, J = 9.51 Hz, 1H), 8.30 (dt, J = 7.80, 1.90 Hz, 1H), 8.02 (dt, J = 7.79, 1.34 Hz, 1H), 7.99 (d, J = 9.57 Hz, 1H), 7.86 (d, J = 8.50 Hz, 2H), 7.69 (t, J = 7.8 Hz, 1H), 3.52 – 3.46 (m, 4H), 3.29 (s, 3H), 2.81 (s, 3H); ^{13}C-NMR δ_C (151 MHz, DMSO-d_6) 166.25, 151.38, 145.82, 140.14, 135.75, 135.63,

134.98, 131.13, 130.06, 129.80, 129.53 (2C), 127.18 (2C), 127.15, 127.07, 126.33, 124.63, 116.93, 71.01, 58.45, 43.64, 42.78; LC-MS, APCI$^+$: *m/z* $[M + H]^+$ = 417.1, calculated exact mass = 416.1307, purity = 99%, t_r = 2.57 min.

N-(1-Hydroxybutan-2-yl)-3-(3-(4-(methylsulfinyl)phenyl)imidazo[1,2-b]pyridazin-6-yl)benzamide ***(23)***. Purified by prep-TLC (developed once in 3% EtOH/DCM, once in 6% EtOH/DCM and once in 8% EtOH/DCM). Yellow solid (0.0039 g, 13%); R_f (CH_3OH : CH_2Cl_2 10 : 90) = 0.35; ^{1}H-NMR δ_H (300 MHz, DMSO-d_6) 8.59 (t, *J* = 1.10 Hz, 1H), 8.50 (d, *J* = 8.44 Hz, 2H), 8.44 (s, 1H), 8.40 (d, *J* = 9.55 Hz, 1H), 8.32 (dt, *J* = 7.85, 1.25 Hz, 1H), 8.25 (dt, *J* = 8.34, 1.65 Hz, 1H), 8.07 – 8.00 (m, 2H), 7.87 (d, *J* = 8.44 Hz, 2H), 7.70 (t, *J* = 7.79 Hz, 1H), 4.70 (t, *J* = 5.69 Hz, 1H), 3.94 (m, 1H), 3.49 (dt, *J* = 11.35, 5.80 Hz, 1H), 2.82 (s, 3H), 1.79 – 1.65 (m, 1H), 1.60 – 1.41 (m, 1H), 0.93 (t, *J* = 7.40 Hz, 3H); ^{13}C-NMR δ_C (151 MHz, DMSO-d_6) 166.30, 151.36, 145.83, 140.14, 136.32, 135.45, 134.98, 131.14, 129.87 (2C), 127.21 (2C), 127.16, 127.06, 126.33 (2C), 124.62 (2C), 116.93, 63.56, 53.69, 43.65, 24.17, 11.15; LC-MS, APCI$^+$: *m/z* $[M + H]^+$ = 449.1, calculated exact mass = 448.1569, purity = 99%, t_r = 3.45 min.

N-Cyclopropyl-3-(3-(4-(methylsulfinyl)phenyl)imidazo[1,2-b]pyridazin-6-yl)benzamide ***(24)***. Purified by prep-TLC (developed in 4% CH_3OH/DCM). Yellow solid (0.050 g, 45%); R_f (CH_3OH : CH_2Cl_2 10 : 90) = 0.44; ^{1}H-NMR δ_H (600 MHz, DMSO-d_6) 8.62 (d, *J* = 4.19 Hz, 1H), 8.49 (t, *J* = 1.81 Hz, 1H), 8.46 (d, *J* = 8.54 Hz, 2H), 8.41 (s, 1H), 8.37 (d, *J* = 9.33 Hz, 1H), 8.28 (dt, *J* = 7.8, 1.5 Hz, 1H), 7.99 – 7.95 (m, 2H), 7.84 (d, *J* = 8.58 Hz, 2H), 7.66 (t, *J* = 7.75 Hz, 1H), 2.89 (m, 1H), 2.80 (s, 3H), 0.73 (td, *J* = 7.04, 4.74 Hz, 2H), 0.60 (td, *J* = 15.64, 6.26 Hz, 2H); ^{13}C-NMR δ_C (151 MHz, DMSO-d_6) 167.46, 151.34, 145.83, 140.13, 135.78, 135.56, 134.96, 131.13, 129.98, 129.74, 129.44 (2C), 127.20 (2C), 127.16, 127.06, 126.30 (2C), 116.92, 43.65, 23.58, 6.28 (2C); LC-MS, APCI$^+$: *m/z* $[M + H]^+$ = 417.1, calculated exact mass = 416.1307, purity = 99%, t_r = 2.68 min.

N,N-Dimethyl-3-(3-(4-(methylsulfinyl)phenyl)imidazo[1,2-b]pyridazin-6-yl)benzamide ***(25)***. Purified by prep-TLC (developed once in 3% CH_3OH/DCM and once in 5%

CH_3OH/DCM). Yellow solid (0.011 g, 10%); R_f (CH_3OH : CH_2Cl_2 10 : 90) = 0.48; ^{1}H-NMR δ_H (300 MHz, DMSO-d_6) 8.52 – 8.38 (m, 3H), 8.33 (d, J = 9.41 Hz, 1H), 8.21 (dt, J = 7.43, 1.25 Hz, 1H), 8.13 (s, 1H), 7.95 (d, J = 9.47 Hz, 1H), 7.86 (d, J = 8.00 Hz, 2H), 7.74 – 7.53 (m, 2H), 3.14 – 2.92 (br s, 6H), 2.83 (s, 3H); ^{13}C-NMR δ_C (151 MHz, DMSO-d_6) 169.96, 151.35, 145.81, 140.11, 137.81, 135.63, 134.94, 131.13, 129.76, 129.20 (2C), 128.42 (2C), 127.16, 127.13, 127.01, 126.05 (2C), 124.59, 117.00, 43.63, 26.79; LC-MS, APCI$^+$: *m/z* [M + H]$^+$ = 405.1, calculated exact mass = 404.1307, purity = 97%, t_r = 2.49 min.

*N-Methyl-3-(3-(4-(methylsulfinyl)phenyl)imidazo[1,2-b]pyridazin-6-yl)benzamide (**26**).* Purified by prep-TLC (developed in 0-10% CH_3OH/DCM with a few drops of 7 M aqueous ammonia). Yellow solid (0.019 g, 18%); R_f (CH_3OH : CH_2Cl_2 10 : 90) = 0.40; ^{1}H-NMR δ_H (300 MHz, DMSO-d_6) 8.64 (q, J = 5.14 Hz, 1H), 8.54 (t, J = 2.03 Hz, 1H), 8.48 (d, J = 8.60 Hz, 2H), 8.44 (s, 1H), 8.39 (d, J = 9.52 Hz, 1H), 8.31 (dt, J = 7.80, 1.25 Hz, 1H), 8.05 – 7.94 (m, 2H), 7.87 (d, J = 8.43 Hz, 2H), 7.70 (t, J = 7.76 Hz, 1H), 2.83 (s, 3H); ^{13}C-NMR δ_C (151 MHz, DMSO-d_6) 166.58, 151.44, 145.82, 140.13, 135.85, 134.98, 131.13, 129.97 (2C), 129.82 (2C), 129.29 (2C), 127.18 (2C), 127.09, 126.27 (2C), 124.64, 43.63, 26.79; LC-MS, APCI$^+$: *m/z* [M + H]$^+$ = 391.1, calculated exact mass = 390.1150, purity = 96%, t_r = 2.46 min.

*(3-(3-(4-(Methylsulfinyl)phenyl)imidazo[1,2-b]pyridazin-6-yl)phenyl)(morpholino)methanone (**27**).* Purified by prep-TLC (developed once in 3% CH_3OH/DCM and once in 5% CH_3OH/DCM). Yellow solid (0.060 g, 51%); R_f (CH_3OH : CH_2Cl_2 10 : 90) = 0.51; ^{1}H-NMR δ_H (300 MHz, Methanol-d_4) 8.48 (d, J = 8.7 Hz, 2H), 8.29 (s, 1H), 8.28 – 8.18 (m, 3H), 7.96 – 7.88 (m, 3H), 7.71 (t, J = 8.21 Hz, 1H), 7.64 (dt, J = 7.66, 1.47 Hz, 1H), 3.89 – 3.60 (m, 8H), 2.90 (s, 3H); ^{13}C-NMR δ_C (151 MHz, DMSO-d_6) 168.97, 151.26, 145.88, 140.13, 136.97, 135.77, 134.98, 131.14 (2C), 129.98, 129.29 (2C), 128.65 (2C), 127.19, 127.05, 126.04, 124.61, 117.02, 66.56 (2C), 43.66, 40.55 (2C); LC-MS, APCI$^+$: *m/z* [M + H]$^+$ = 447.1, calculated exact mass = 446.1413, purity = 97%, t_r = 2.61 min.

*(3-(3-(4-(Methylsulfinyl)phenyl)imidazo[1,2-b]pyridazin-6-yl)phenyl)(piperidin-1-yl)methanone (**29**)*. Purified by prep-TLC (developed once in 3% CH_3OH/DCM and once in 5% CH_3OH/DCM). Yellow solid (0.042 g, 36%); R_f (CH_3OH : CH_2Cl_2 10 : 90) = 0.53; ^{1}H-NMR δ_H (300 MHz, Methanol-d_4) 8.48 (d, J = 8.4 Hz, 2H), 8.29 (s, 1H), 8.26 – 8.13 (m, 3H), 7.97 – 7.85 (m, 3H), 7.70 (t, J = 7.70 Hz, 1H), 7.60 (dt, J = 7.66, 1.00 Hz, 1H), 3.86 – 3.70 (m, 2H), 3.53 – 3.40 (m, 2H), 2.90 (s, 3H), 1.81 – 1.54 (m, 6H); ^{13}C-NMR δ_C (151 MHz, Methanol-d_4) 170.16, 151.63, 143.96, 139.97, 137.00, 135.77, 133.10, 131.51, 129.29 (2C), 128.20 (2C), 128.18, 127.57, 127.32, 125.64, 125.11, 123.99, 116.98, 48.74, 43.05, 42.15, 26.25, 25.36, 24.03; LC-MS, APCI$^+$: *m/z* $[M + H]^+$ = 445.1, calculated exact mass = 444.1620, purity = 98%, t_r = 2.69 min.

*N-(4-Methoxycyclohexyl)-3-(3-(4-(methylsulfinyl)phenyl)imidazo[1,2-b]pyridazin-6-yl)benzamide (**30**)*. Purified by prep-TLC (developed once in 3% CH_3OH/DCM and once in 5% CH_3OH/DCM). Yellow solid (0.058 g, 45%); R_f (CH_3OH : CH_2Cl_2 10 : 90) = 0.65; ^{1}H-NMR δ_H (300 MHz, DMSO-d_6) 8.55 (t, J = 1.77 Hz, 1H), 8.49 (d, J = 8.23 Hz, 2H), 8.44 (s, 1H), 8.39 (d, J = 9.56 Hz, 1H), 8.32 (dt, J = 8.26, 0.83 Hz, 1H), 8.05 – 7.96 (m, 2H), 7.87 (d, J = 8.12 Hz, 2H), 7.69 (t, J = 7.76 Hz, 1H), 3.93 – 3.74 (m, 1H), 3.27 (s, 3H), 3.23 – 3.08 (m, 1H), 2.83 (s, 3H), 2.14 – 2.00 (m, 2H), 2.01 – 1.85 (m, 2H), 1.51 – 1.33 (m, 2H), 1.33 – 1.14 (m, 2H); ^{13}C-NMR δ_C (151 MHz, DMSO-d_6) 165.76, 151.36, 146.05, 140.16, 136.40, 135.53, 134.92, 131.20, 129.80 (2C), 129.62, 129.55 (2C), 127.28 (2C), 127.00, 126.35, 124.59, 116.83, 78.29, 55.51 (2C), 48.57 (2C), 43.75, 30.68, 30.42; LC-MS, APCI$^+$: *m/z* $[M + H]^+$ = 489.2, calculated exact mass = 488.1882, purity = 95%, t_r = 2.35 min.

*N-(2-(Methylamino)ethyl)-3-(3-(4-(methylsulfinyl)phenyl)imidazo[1,2-b]pyridazin-6-yl)benzamide (**21**)*. Purified by prep-TLC (developed in 0-10% CH_3OH/DCM with a few drops of 7 M aqueous ammonia). Pale yellow solid (0.015 g, 30%); R_f (CH_3OH : CH_2Cl_2 3 : 97) = 0.25; ^{1}H-NMR δ_H (300 MHz, Methanol-d_4) 8.55 (s, 1H), 8.26 (dd, J = 8.3, 1.1 Hz, 1H), 8.17 - 8.06 (m, 4H), 8.01 (dd, J = 7.6, 1.4 Hz, 1H), 7.83 (d, J = 9.6 Hz, 1H), 7.66 (t, J = 7.8 Hz, 1H),

7.41 (d, J = 8.7 Hz, 2H), 3.71 (t, J = 5.9 Hz, 2H), 3.13 (t, J = 6.0 Hz, 2H), 2.68 (s, 3H), 2.56 (s, 3H); ^{13}C-NMR δ_C (101 MHz, Methanol-d_4) 168.80, 151.21, 139.18, 135.84, 134.61, 131.70 (2C), 129.96, 129.09 (2C), 128.52, 126.84 (3C), 125.97 (2C), 125.34, 124.72, 115.99, 49.78, 40.88, 37.36, 33.31; LC-MS, APCI$^+$: *m/z* $[M + H]^+$ = 434.53, calculated exact mass = 433.1572, purity = 99.9%, t_r = 2.017 min.

2.0 Biological and Solubility Evaluation

***In vitro* Asexual Blood Stage Antiplasmodium Testing.** A modified [^{3}H]-hypoxanthine incorporation assay[1] was used to screen compounds **5**, **7** – **12**, **14**, **17** and **18** against multidrug resistant (K1) and sensitive (NF54) strains of *P. falciparum in vitro*. A variation of the medium previously described[2,3] consisting of RPMI 1640 supplemented with 0.5% ALBUMAX® II, 25 mM Hepes, 25 mM $NaHCO_3$ (pH 7.3), 0.36 mM hypoxanthine and 100 μg/mL neomycin was used to cultivate *P. falciparum* parasites. Human erythrocytes served as host cells. Humidified modular chambers at 37 °C with an atmosphere of 3% O_2, 4% CO_2 and 93% N_2 were used to maintain cultures. DMSO was used to dissolve the compounds (10 mg/mL) with the aid of sonication after which the stock solutions were diluted in hypoxanthine-free culture medium. To each drug titrated in 100 μL duplicates over a 64-fold range, infected erythrocytes (100 μL per well with 2.5% hematocrit and 0.3% parasitemia) were added. 0.5 μCi of [^{3}H]hypoxanthine in 50 μL medium was then added after 48 hours incubation, and plates were incubated for an additional 24 hours. The radioactivity of the parasites harvested onto glass-fiber filters was recorded using a Betaplate liquid scintillation counter (Wallac, Zurich). At each drug concentration, the results were recorded as counts per minute (cpm) per well and expressed as a percentage of the untreated controls. Linear interpolation was used to estimate fifty percent inhibitory concentrations (IC_{50}).[4]

The parasite lactate dehydrogenase assay using a modified method described by Makler *et al*[5] was used to quantitatively assess the *in vitro* antiplasmodium activity of compounds **6**,

13, **15**, **16**, **19** – **30** and **3b**. The chloroquine sensitive strain of *P. falciparum* (NF54) was used to test the test samples in triplicate on two occasions. A modified method of Trager and Jensen[3] was used to maintain continuous *in vitro* cultures of asexual erythrocyte stages of *P. falciparum*. DMSO was used to dissolve (with sonication) test samples to prepare 20 mg/mL stock solutions which were kept at – 20 °C until required. If not completely dissolved, samples were tested as a suspension. On the day of the experiment, further dilutions were prepared. In all experiments, chloroquine and artesunate were used as reference drugs. To determine the IC_{50} values, a full dose response was performed for all the compounds 72 hours post-incubation. 10 concentrations were obtained by serially diluting the test samples 2-fold. A starting concentration of 1000 ng/mL was used to test control compounds. Parasite viability was not affected to any measurable extent by the highest concentration of solvent they were exposed to. A non-linear dose-response curve fitting analysis via Graph Pad Prism v.4.0 software was used to obtain the IC_{50} values.

***In vitro* Gametocidal Screening**. Early-stage (> 95% stage II/III) and late-stage (> 95% stage IV/V) gametocytes (2% gametocytemia, 2% hematocrit) were generated from a *P. f* NF54-*pfs16*-GFP-Luc line, and incubated for 48 h under drug pressure with hypoxic conditions at 37 °C.[6] IC_{50} values were determined using a luciferase reporter assay as previously described.[6]

Male Gamete Exflagellation Inhibition Assay (EIA). The EIA was performed by inducing gametogenesis on a > 98% stage V gametocyte population with 100 μM xanthurenic acid (XA, Sigma Aldrich), in ookinete medium (RPMI 1640 with 25 mM HEPES, 0.2% sodium bicarbonate, pH 8.0, and 20% human serum) followed by a > 15 min incubation at room temperature. Exflagellating centers were recorded by video using a Carl Zeiss NT 6V/10W Stabmicroscope with a MicroCapture camera, at 10x magnification in a Neubauer chamber at room temperature. Centers were semi-automatically quantified from 15 randomly located videos of 8-10 s each between 15-22.5 min after gametogenesis induction.[7]

***In vitro Pv*PI4K Inhibition Assays.** Full-length *Pv*PI4K (PVX_098050) recombinant protein was expressed in a baculovirus-insect cell expression system and purified as previously described.[8] *Pv*PI4K kinase inhibition assays were performed based on previously described methods[8,9] and the ADP-Glo assay kit (Promega) was used to measure ADP formation. L-alpha-phosphatidylinositol (PI; Avanti Polar Lipid, cat. 840042P) dissolved in 3% n-Octylglucoside to a stock concentration of 20 mg/ml was used as the lipid substrate. Briefly, final kinase reactions contained ~8 nM purified *Pv*PI4K (or ~2 nM *Pv*PI4K for IC_{50} determination of Compound **1**), 10 μM ATP, 0.1 mg/mL PI, 0.1% DMSO, +/- inhibitor in assay buffer (25 mM HEPES pH 7.4, 100 mM NaCl, 3 mM $MgCl_2$, 1 mM DTT, 0.025 mg/ml BSA, 0.2% Triton-X-100). Reactions were initiated by the addition of *Pv*PI4K and incubated for 40 minutes at 22 °C. ADP formation was measured using the ADP-Glo kinase kit (Promega) according to manufacturer's instructions. Briefly, 4 μL ADP-Glo reagent (containing 10 mM $MgCl_2$ for *Pv*PI4K assays) was added to 4 μL kinase reaction in white 384 shallow well plates (Nunc, Cat no. 264706) and incubated for 40 minutes at 22 °C to deplete the remaining ATP. 8 μL of Kinase Detection Reagent was then added and the reaction was incubated for a further 40 minutes at 22 °C. Luminescent signal was measured using the EnSpire Multimode Plate Reader (PerkinElmer) with crosstalk correction. Data were normalized based on the DMSO controls (no inhibitor, 100% activity) and the 100% inhibition controls. Reactions were carried out in triplicate and percentage inhibition was calculated based on the average of two independent experiments.

***In vitro Pf*PKG Inhibition Assays.** Full length *Pf*PKG (PF3D7_1436600) was expressed in *Escherichia coli* and purified as previously described.[10,11] *Pf*PKG kinase inhibition assays were performed based on previously described methods using ADP-Glo assay to measure ADP formation.[11,12] Briefly, final kinase reactions contained ~1 nM purified *Pf*PKG protein, 10 μM ATP, 20 μM peptide substrate GRTGRRNSI-NH2 (Sigma-Aldrich, Cat no. SCP0212), 0.1% (v/v) DMSO, +/- inhibitor in assay buffer (25 mM HEPES pH 7.4, 0.01% (w/v) BSA, 0.01%

(v/v) Triton-X 100, 20 mM $MgCl_2$, 2 mM DTT, 10 μM cGMP). Reactions were initiated by the addition of *Pf*PKG and incubated for 30 minutes at 22 °C (resulting in ~10% ATP conversion). ADP formation was measured using the ADP-Glo Kinase Kit (Promega) according to manufacturer's instructions and data was analysed as described for the *Pv*PI4K inhibition assays above.

***In vitro Hu*PI4KIIIβ Inhibition Assays.** *Hu*PI4KIIIβ (Q9UBF8) inhibition assays were performed by Reaction Biology Corp. using the ADP-Glo kinase assay format. Reactions were carried out at 10 μM ATP and 100 μM PI. Compounds were tested at a single dose of 1 μM in duplicate.

***In silico* Modelling.** *Protein Preparation and Docking Grid Generation*. A *Pf*PI4k homology model[13] was selected for *Pf*PI4K docking while the *Pv*PKG PDB structure 5EZR[10] was selected for *Pf*PKG docking. The *Pf*PI4K homology model had been previously prepared for docking while the 5EZR PDB structure (full-length *Pv*PKG with small molecule inhibitor ML10 bound within the ATP-binding site) was prepared for docking using the Maestro Protein Preparation Wizard[14] from the Schrodinger2020-1 (Schrödinger Release 2020-1: Maestro, Schrödinger, LLC, New York, NY, 2020) release. Under the Protein Preparation Wizard's import tab, the protein preprocess was run with the "assign bond order," "add hydrogens," "create disulfide bonds," "fill in missing side chains using Prime" and "generate het states using Epik" at pH 7.0 +/- 2.0 options selected. The only problems reported by the preprocess protein report were two residues (S168 and N401) with alternate positions saved to the original PDB file. S168 being a surface residue was committed arbitrarily to the position with an occupancy of 0.6 while N401 was committed to a position where it could form a H-bond with the proximal N476. The prepared structure was then reviewed under the review and modify tab where five possible protonation states for the ML10 ligand were examined. The zwitterionic protonation state S2 was selected for the ML10 ligand with a protonated dimethyl amine and a deprotonated sulfonamide forming salt-bridge interactions with the charged E618 and K563

respectively. Under the refine tab, the H-bond assignments were optimised using the automated H-bond optimisation with the PROPKA set to pH 7.0. After the H-bond optimisation, all waters more than 3.0 Å away from het groups were removed. A restrained minimisation was then run with a heavy atom convergence set to an RMSD of 0.30 Å using the OPLS3e[15] forcefield.

Docking grids were then generated for the *Pf*PI4K model and the prepared *Pv*PKG structures using the Glide[16–18] Receptor Grid Generation application. In both structures, the receptor was defined as a region around the ligand (ML10 for *Pv*PKG and MMV390048 for *Pf*PI4K). The van der Waals radius scaling factor was left as default (1.0) with a partial charge cut-off of 0.25. The grid centre was set to the centroid of the receptor ligand and the grid size was set to a "size similar to the receptor ligand." An H-bond donor constraint from the backbone amide of hinge (*Pf*PI4K – V1357; *Pv*PKG – V614) region was added for each receptor. No rotatable groups or excluded volumes were included in the grid generation panel. Docking grids were then generated for each receptor.

Ligand Docking. The set of SFK52 imidazopyridazine ligands from this study were prepared using the Maestro's LigPrep tool. Ionisation was set to generate all ionisation states in a pH range of 7.0 +/- 1.0 using the Epik[19,20] algorithm with the desalt and generate tautomer options selected. The option to retain all specified tautomers and vary other chiral centres was set. The 3D ligand structures with protonation states expected at biological pH were then generated. The output was then visually inspected and most compounds in this set gave rise to two enantiomers on account of the unspecified sulfoxide stereocentre.

The prepared set of ligands was then docked into the respective docking grids for *Pf*PI4K and *Pv*PKG using Glide Ligand Docking. In the Ligand docking panel, the van der Waal radii scaling factor was set to 0.80 with a partial charge cut-off of 0.15. Docking was run at the standard precision (SP) setting with flexible ligand sampling set to sample nitrogen inversions and ring conformations. A bias sampling of torsions for all predefined functional groups was

set. The add Epik state penalty to docking score box was selected. The H-bond constraint parameter from each docking grid was implemented ensuring every output ligand pose contained that H-bond. The output was then set to write out only one pose per ligand.

Post Docking Energy Minimisation and MMGBSA Scoring. The docking outputs were visually inspected. Ligands with reasonable poses were submitted for minimisation and molecular mechanics generalised Born surface area (MMGBSA) free energy of binding (MMGBSA ΔG_{bind}) calculations. MMGBSA calculations were conducted using Prime[21]. The VSGB implicit solvation model was selected using the OPLS3e forcefield. Flexible residues were defined as all residues within 5.0 Å of the docked ligand. The hierarchical sampling method was selected. Both the final protein-ligand pose and the MMGBSA score were used to evaluate the binding of each ligand to both the *Pf*PI4K and *Pv*PKG proteins.

***In vitro* hERG Testing.** The hERG inhibition studies were carried out using a QPatch hERG assay employing a four-point concentration-response format by the UK-based Metrion Biosciences Ltd. The CHO cell line grown and passaged under standard culture conditions was used to stably express the hERG gene. The following compositions for the external (e) and internal (i) recording solutions were used (mM): NaCl – 140 (e) : 0 (i); KCl – 2 (e) : 70 (i); KF - 0 (e) : 60 (i); HEPES - 10 (e) : 10 (i); $MgCl_2$ - 1 (e) : 0 (i); $CaCl_2$ - 2 (e) : 0 (i); Glucose - 5 (e) : 0 (i); EGTA - 0 (e) : 5 (i); Mg_2ATP - 0 (e) : 5 (i) and pH – 7.4 (NaOH) (e) : 7.2 (KOH) (i). During recording, the external recording solution was maintained at room temperature. This solution was also prepared regularly and stored at 4 °C until required. The internal recording solution was prepared and stored at – 20 °C until needed.

The QPatch is an automated chip-based planar patch clamp method. A Giga-ohm seal between the membrane surface and a treated silicon surface is created by drawing cells added to each well across a small aperture using suction. To a reservoir on the chip is added a small volume of bathing solution containing the test compound or control bathing solution which perfuses across the cell through quartz-lined microfluidic channels. Before the next sample is

added, the solution is removed by capillary action. From a holding potential of 90 mV, and at a stimulus frequency of 0.1 Hz, currents were triggered using the industry + 40/- 40 voltage protocol.

Concentration-response curves were established by cumulatively adding four escalating concentrations of the test compounds to an individual cell. To do this, the whole-cell configuration was firstly allowed to be achieved. Secondly, the vehicle (0.1% DMSO v/v in external recording solution) was added to each well in two bolus additions allowing a two-minute recording time between each addition. The four concentrations (0.3 – 10 μM) of test compounds were then added in two bolus additions at 2-minute intervals. During the 4-minute recording time, the effect on the hERG tail current amplitude was measured. The final concentration of DMSO for all the concentrations (0.3, 1, 3 and 10 μM) of the test samples was 0.1% v/v in the external recording solution. The experiments at each concentration were done in triplicate for each compound. The percent inhibition, as a reduction in mean peak current relative to the value measured at the end of the vehicle control period, was calculated with the aid of a bioinformatics suite developed and running in Pipeline Pilot (Biovia, USA). The concentration-response curves, which enabled calculation of the IC_{50} values, were constructed from the obtained percent inhibition data. Extrapolated IC_{50} values are reported for compounds which could not achieve 50% inhibition even at the highest tested concentration of 10 μM.

***In vitro* Cytotoxicity Assay.**[22] Cytotoxicity was measured using the MTT-assay which measures cellular growth and survival calorimetrically. All growth and chemosensitivity was measured by the formation of tetrazolium salt. The test samples were assayed in triplicate on one occasion. Stock solutions of 2 mg/mL of test samples in DMSO were prepared with poorly soluble samples being tested as suspensions. The test samples were kept at -20 °C until required. In all experiments, emetine was used as a reference drug. 10-fold serial dilutions in complete medium to give 6 concentrations were made from an initial concentration of 100 μg/mL with the lowest concentration being 0.001 μg/mL. The cell viability was not affected

by the highest concentration of the solvent to which the cells were exposed. The full dose-response curves plotted using a non-linear dose-response curve fitting analysis via GraphPad Prism V 4 software enabled the determination of the IC_{50} values.

Solubility Determination. The solubilities of compounds **5** – **12**, **19**, **21**, **26** – **28** and **3b** were determined using a miniaturised shake flask method.[23] Calibration standards (10 - 220 μM in DMSO) were prepared from 10 mM stock solutions of the test compounds in DMSO. Duplicate aqueous samples in phosphate buffered saline (pH 6.5) were spiked (1:50) with 10 mM stock solutions. After drying off the DMSO in a GeneVac (MiVac, 90 min, 37 °C), the samples were incubated while shaking for 20 hours at 25 °C. The solutions were then filtered, and their absorbance recorded using HPLC-DAD (Agilent 1200 Rapid Resolution HPLC with a diode array detector). Calibration curves were plotted from the prepared calibration standards, which enabled the determination of solubility of aqueous samples.

For compounds **14**, **16** – **18**, **20**, **22**, **24**, **29** and **30**, kinetic (turbidimetric) solubility[24] assay was used to determine solubility. In this method, one intact PBS buffer tablet was dissolved in 1 L of water to make a phosphate buffered saline (PBS) solution constituting 0.14 M NaCl, 0.003 M KCl and 0.01 M phosphate buffer (pH 7.4). The solution was then filtered through a 0.22 μm nylon filter to remove particulate contaminants. The pH was then verified using a pH meter. Test compounds were dissolved in DMSO to give 10 mM stock solutions. Starting from 8 mM to 0.25 mM (also referred to as predilution), serial dilutions of the compounds in DMSO were prepared in triplicate on a 96-well plate. A secondary dilution plate containing 196 μL DMSO and PBS buffer in each well of the first six and last six columns of the 96-well plate respectively was prepared. By pipetting 4 μL aliquots from the predilution plate to corresponding wells in the secondary plate containing 196 μL DMSO and PBS buffer (final volume of 200 μL in each well), secondary serial dilutions (5 – 200 μM) in DMSO and PBS buffer, also in triplicate, were prepared. The DMSO serial dilutions served as controls to ensure the test compounds in solution did not absorb electromagnetic radiation at the test

wavelength. The plate was covered, placed in an oven maintained at 26 °C and left to incubate for 2 hours. A UV-Visible Multiskan Go 1510-05438 spectrometer (Thermo Scientific) was then used to measure the absorbance values of the wells. The absorbance of the blank wells containing only DMSO and 2% DMSO in PBS were then subtracted from the absorbance values of cells containing the samples to get corrected values. Employing excel, the corrected absorbance values were plotted as a function of concentration. For a compound soluble at all concentrations, a constant absorbance value of 0 at all concentrations is observed. For insoluble compounds, the precipitate formed at a certain concentration causes turbidity, the absorbance of which was measured by a UV-Visible spectrometer. The concentration above which the test compound precipitates from solution causing a sustained upward deviation of absorbance values from zero was taken to be the solubility value.

3.0 Supplementary Tables S1, S2 and S3

Table S1. *In vitro* Asexual Blood Stage Antiplasmodium Activity against *P. falciparum* (NF54 and K1) of some Analogues

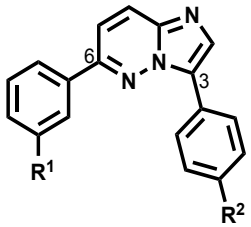

Code	R^1	R^2	*P. f* IC_{50}, µM[a,b]	
			NF54	K1
5	**SOMe**	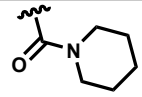	0.317	0.284
6	**SOMe**	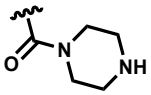	0.103	
7	**SOMe**	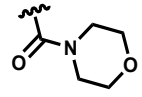	0.162	0.164
8	**SOMe**	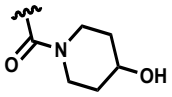	0.106	0.084
9	**SOMe**	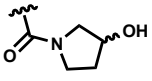	0.055	0.04

Table S1. *In vitro* Asexual Blood Stage Antiplasmodium Activity against *P. falciparum* (NF54 and K1) of some Analogues "continued"

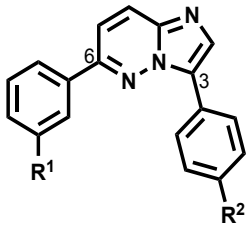

Code	R^1	R^2	*P. f* IC_{50}, µM[a,b]	
			NF54	K1
10	**SOMe**	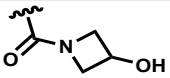	0.097	0.085
11	**SOMe**	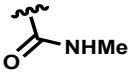	0.067	0.0515
12	**SOMe**	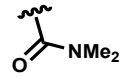	0.146	0.123
13	**SOMe**	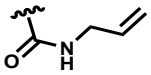	0.141	
14	**SOMe**	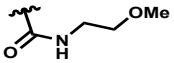	0.144	0.136
15	**SOMe**	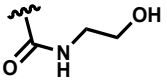	0.371	
16	**SOMe**	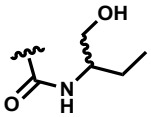	0.290	
17	**SOMe**	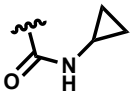	0.209	0.181
18	**SO_2Me**	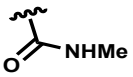	0.019	0.017

[a]Mean from n ≥ 2 independent experiments (Individual IC_{50} values differed by ≤ 2-fold).

[b]Artesunate [IC_{50} = 4.0 nM (NF54), 3.0 nM (K1)] and chloroquine [IC_{50} = 16 nM (NF54), 194 nM (K1)] were used as reference drugs.

Blank cells = data not available

Table S2. *In vitro* Asexual Blood Stage Antiplasmodium Activity against *P. falciparum* NF54, hERG Activity and Cytotoxicity of some Analogues

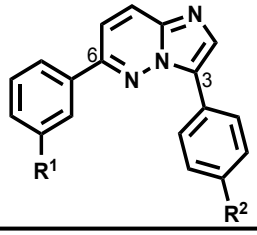

Code	R^1	R^2	*P. f* IC_{50}, µM NF54	hERG activity		Cytotoxicity,[f] CHO cells	
				IC_{50}, µM (SD)[d]	SI[e]	IC_{50}, µM	SI[g]
5	**SOMe**	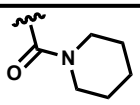	0.317	9.01 (0.66)	28	83	275
7	**SOMe**	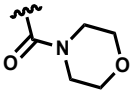	0.162	23.4 (3.69)	144	185	1360
8	**SOMe**	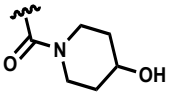	0.106	36.0 (5.26)	340	> 217	> 2067
9	**SOMe**	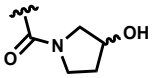	0.055	30.4 (2.12)	553		
10	**SOMe**	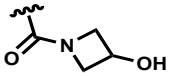	0.097	20.9 (3.56)	215	> 231	> 2381
11	**SOMe**		0.067	17.9 (0.27)	267	75.5	1127
12	**SOMe**	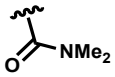	0.146	20.3 (4.19)	139	165	932
21	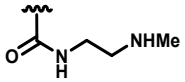	**SOMe**	0.088	30 (0)	341		
26	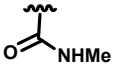	**SOMe**	0.012	30 (0)	2500		
27	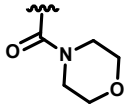	**SOMe**	0.016	30 (0)	1900		
28	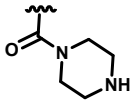	**SOMe**	0.024	30 (0)	1200		

[d]Mean from n = 3 independent experiments; SD, standard deviation; Verapamil was used as a positive control (IC_{50} = 0.560 ± 0.0961 µM).

[e]SI = selectivity index = IC_{50} (hERG)/IC_{50} (*P. f* NF54).

[f]Mean from n = 3 independent experiments; SD, standard deviation; Emetine was used as a reference drug (IC_{50} = 0.033 ± 0.006 µM).

[g]SI = selectivity index = IC_{50} (CHO)/IC_{50} (*P. f* NF54).

Blank cells = data not available

Table S3. *In vitro* % Inhibition of *P. falciparum* Early- and Late-Stage Gametocytes for some Analogues

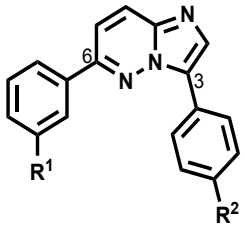

Code	R^1	R^2	% *P. f* EG inh. @ 1 µM (SD)[k]	% *P. f* EG inh. @ 5 µM (SD)[k]	% *P. f* LG inh. @ 1 µM (SD)[k]	% *P. f* LG inh. @ 5 µM (SD)[k]
13	**SOMe**	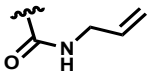	23.9 (2.1)	70.9 (3.0)	73.5 (2.7)	94.5 (3.5)
14	**SOMe**	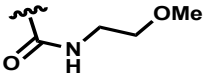	39.5 (15.2)	57.9 (11.2)	53.4 (10.1)	91.4 (1.7)
15	**SOMe**	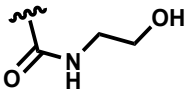	19.2 (5.2)	61.7 (2.6)	68.8 (4.8)	90.5 (3.7)
16	**SOMe**	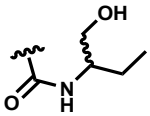	6.3 (8.9)	41.9 (11.7)	44.7 (6.8)	80.7 (2.8)
17	**SOMe**	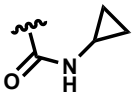	41.0 (11.6)	48.8 (6.2)	34.3 (1.9)	79.8 (4.1)
18	**SO_2Me**	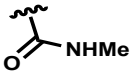	84.9 (1.0)	96.4 (0.6)	98.4 (0.8)	99.5 (0.2)
20	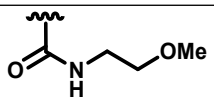	**SOMe**	38.5 (2.6)	70.3 (2.0)	79.2 (4.5)	95.7 (1.0)
22	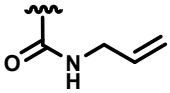	**SOMe**	62.3 (10.1)	72.7 (7.0)	80.3 (3.1)	94.9 (0.6)
24	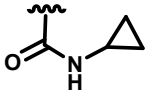	**SOMe**	53.4 (15.0)	67.4 (7.5)	62.7 (5.6)	94.1 (0.8)
28	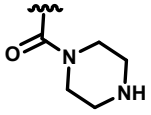	**SOMe**	83.3 (3.4)	78.5 (3.2)	95.4 (0.3)	96.7 (0.3)
29	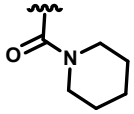	**SOMe**	88.6 (3.0)	86.4 (2.6)	96.2 (0.5)	97.6 (0.6)

[k] Percentage EG and LG inhibition, n = 1, carried out in triplicate.

4.0 ^{1}H-NMR Spectra of Selected Compounds

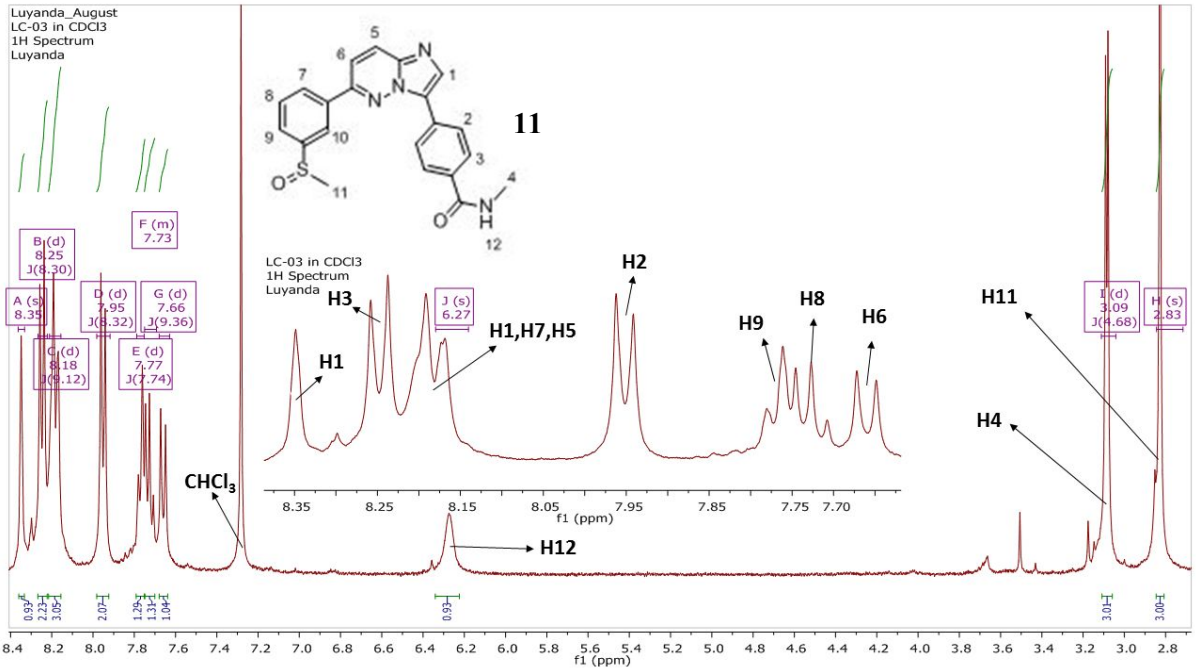

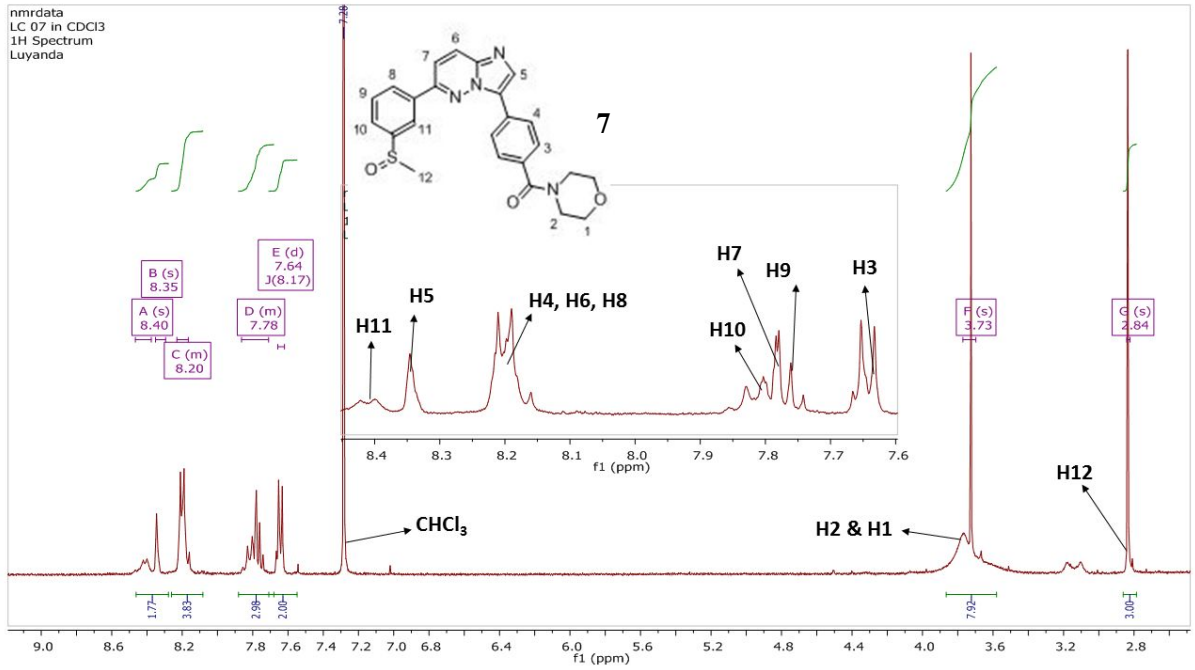

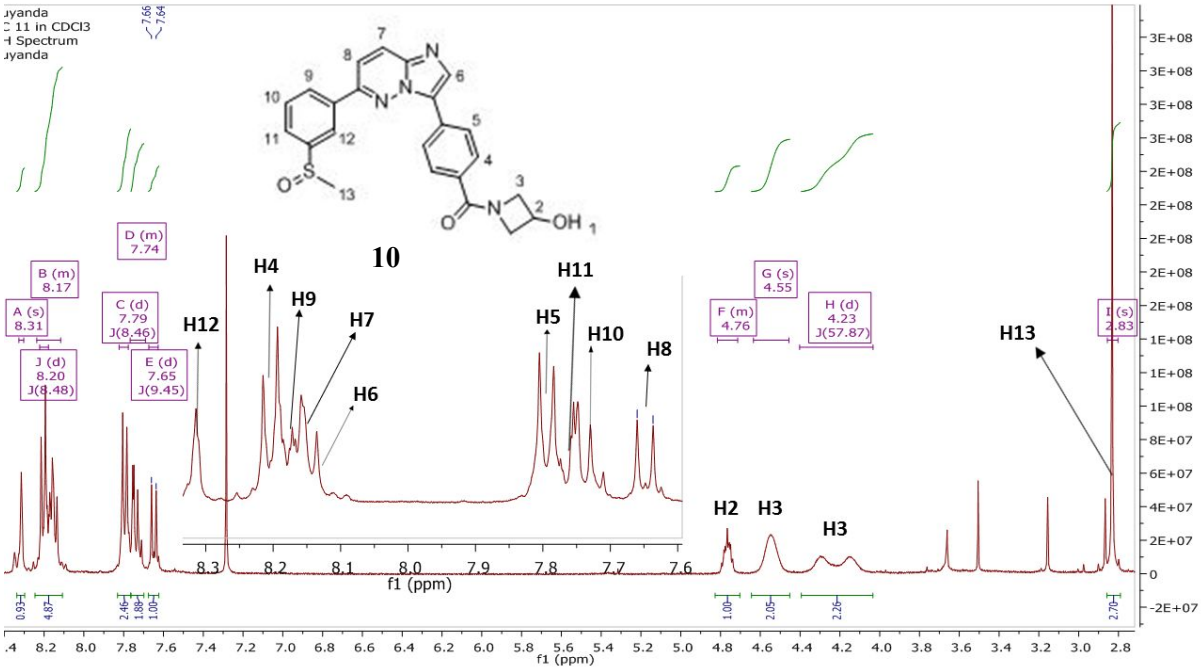
10
A (s) 8.31
B (m) 8.17
C (d) 7.79 J(8.46)
D (m) 7.74
E (d) 7.65 J(9.45)
J (d) 8.20 J(8.48)
F (m) 4.76
G (s) 4.55
H (d) 4.23 J(57.87)
I (s) 2.83
H12
H4
H9
H7
H6
H5
H11
H10
H8
H2
H3
H3
H13
f1 (ppm)

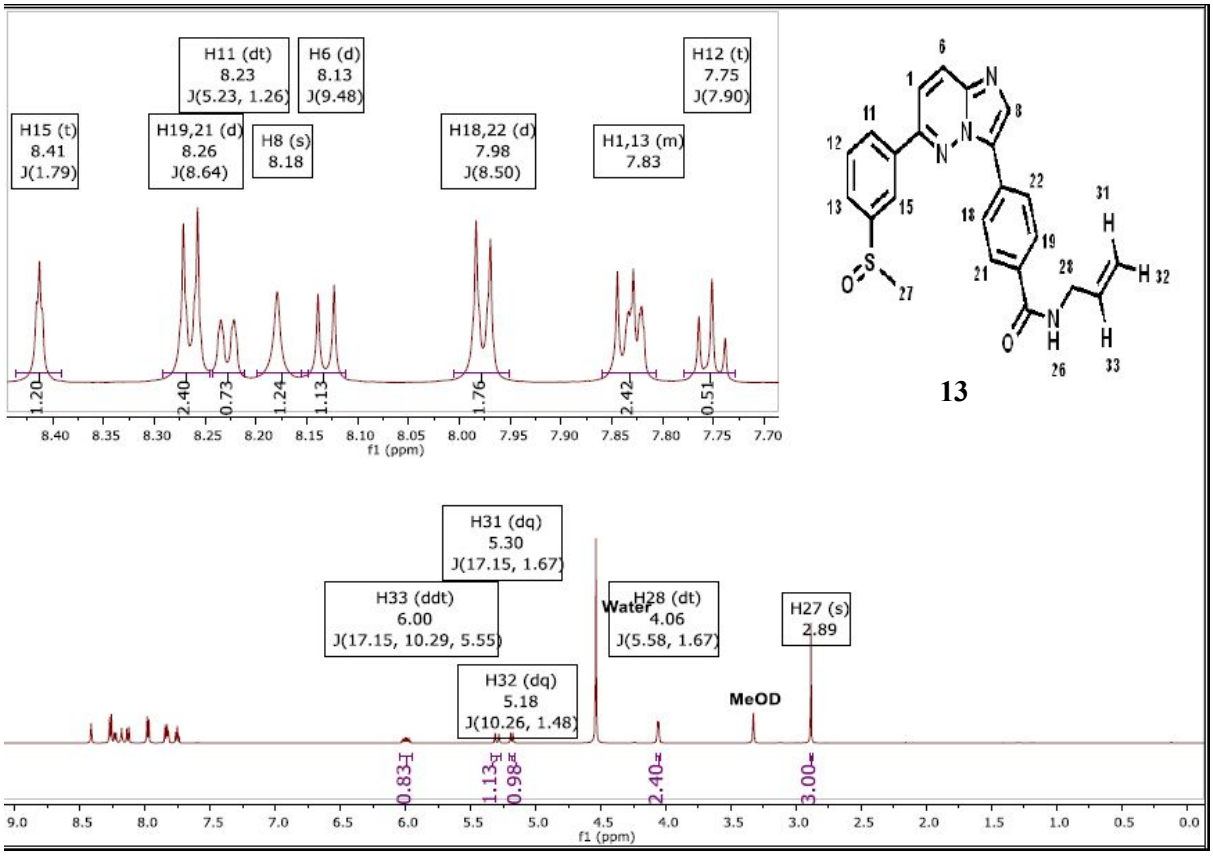
H15 (t) 8.41 J(1.79)
H11 (dt) 8.23 J(5.23, 1.26)
H6 (d) 8.13 J(9.48)
H19,21 (d) 8.26 J(8.64)
H8 (s) 8.18
H18,22 (d) 7.98 J(8.50)
H1,13 (m) 7.83
H12 (t) 7.75 J(7.90)
1.20
2.40
0.73
1.24
1.13
1.76
2.42
0.51
f1 (ppm)
13
H31 (dq) 5.30 J(17.15, 1.67)
H33 (ddt) 6.00 J(17.15, 10.29, 5.55)
H32 (dq) 5.18 J(10.26, 1.48)
Water
H28 (dt) 4.06 J(5.58, 1.67)
MeOD
H27 (s) 2.89
0.83
1.13
0.98
2.40
3.00
f1 (ppm)

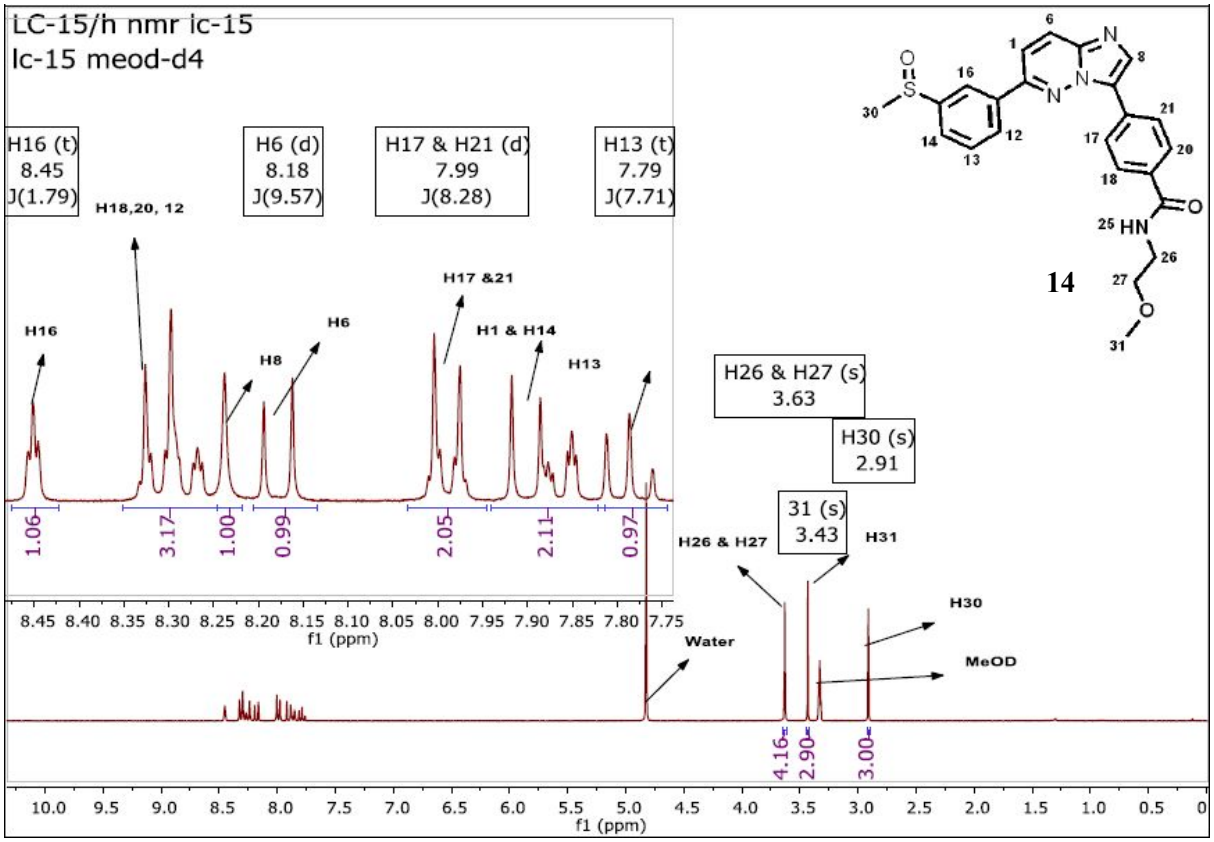
LC-15/h nmr lc-15
lc-15 meod-d4
H16 (t)
8.45
J(1.79)
H18,20, 12
H6 (d)
8.18
J(9.57)
H17 & H21 (d)
7.99
J(8.28)
H13 (t)
7.79
J(7.71)
H16
H8
H6
H17 &21
H1 & H14
H13
1.06
3.17
1.00
0.99
2.05
2.11
0.97
H26 & H27 (s)
3.63
H30 (s)
2.91
31 (s)
3.43
H26 & H27
H31
H30
MeOD
Water
4.16
2.90
3.00
f1 (ppm)
14

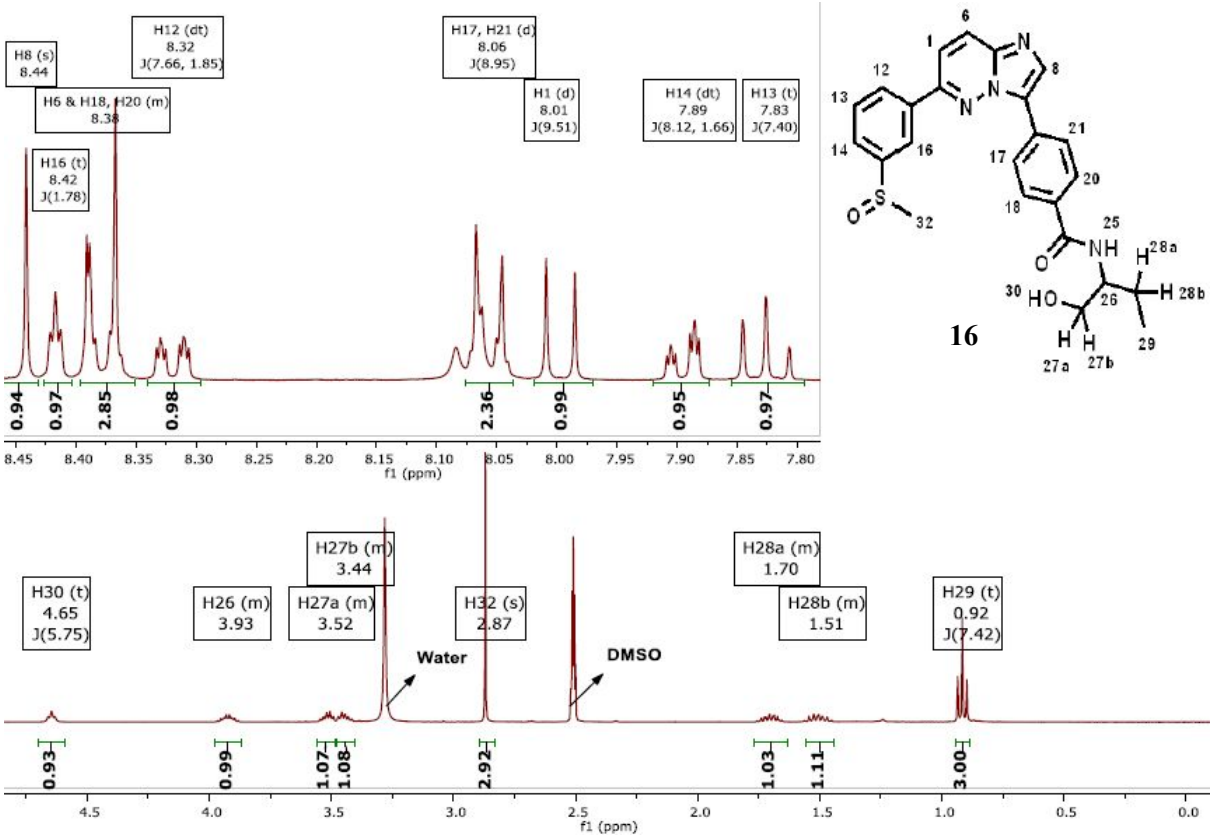
H8 (s)
8.44
H12 (dt)
8.32
J(7.66, 1.85)
H6 & H18, H20 (m)
8.38
H16 (t)
8.42
J(1.78)
H17, H21 (d)
8.06
J(8.95)
H1 (d)
8.01
J(9.51)
H14 (dt)
7.89
J(8.12, 1.66)
H13 (t)
7.83
J(7.40)
0.94
0.97
2.85
0.98
2.36
0.99
0.95
0.97
f1 (ppm)
16
H30 (t)
4.65
J(5.75)
H26 (m)
3.93
H27a (m)
3.52
H27b (m)
3.44
H32 (s)
2.87
Water
DMSO
H28a (m)
1.70
H28b (m)
1.51
H29 (t)
0.92
J(7.42)
0.93
0.99
1.07
1.08
2.92
1.03
1.11
3.00
f1 (ppm)

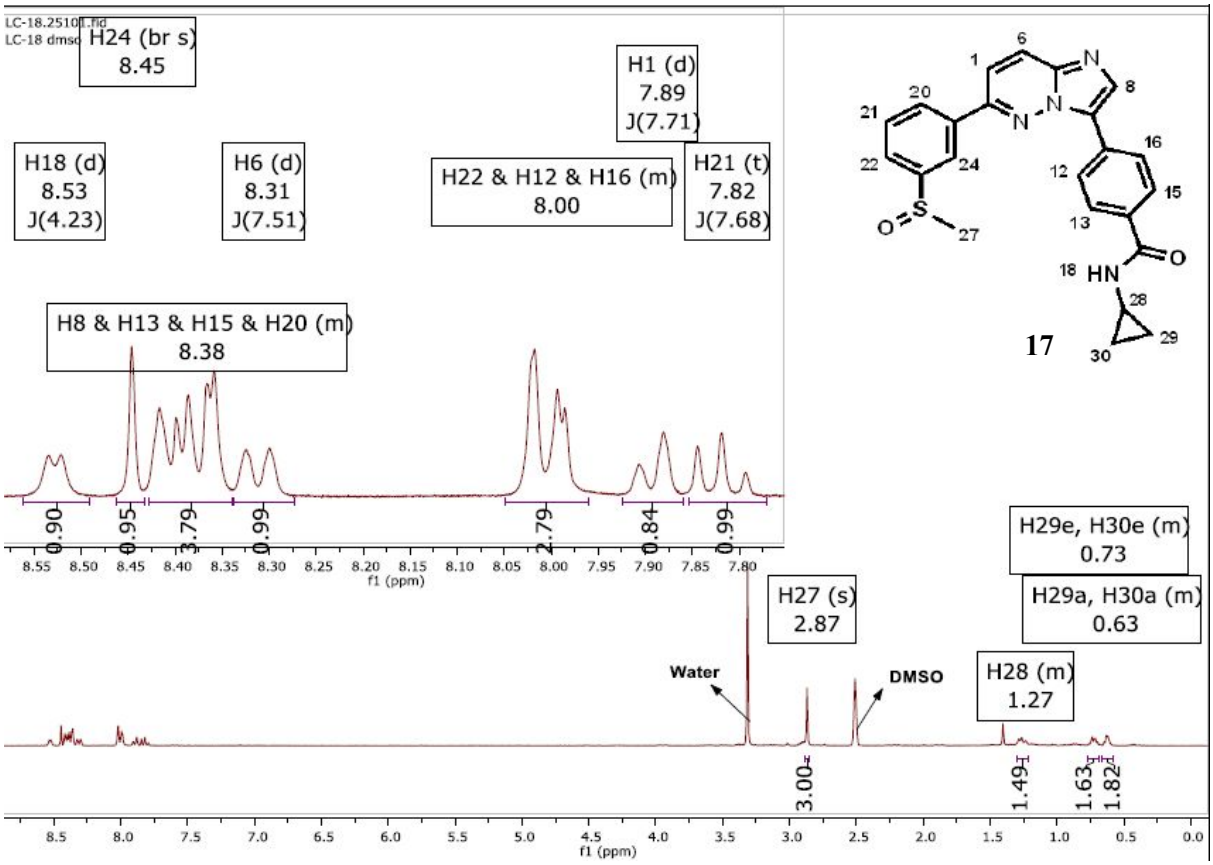
LC-18.2510.1.fid
LC-18 dmso
H24 (br s)
8.45
H1 (d)
7.89
J(7.71)
H18 (d)
8.53
J(4.23)
H6 (d)
8.31
J(7.51)
H22 & H12 & H16 (m)
8.00
H21 (t)
7.82
J(7.68)
H8 & H13 & H15 & H20 (m)
8.38
17
H29e, H30e (m)
0.73
H27 (s)
2.87
H29a, H30a (m)
0.63
Water
DMSO
H28 (m)
1.27
f1 (ppm)

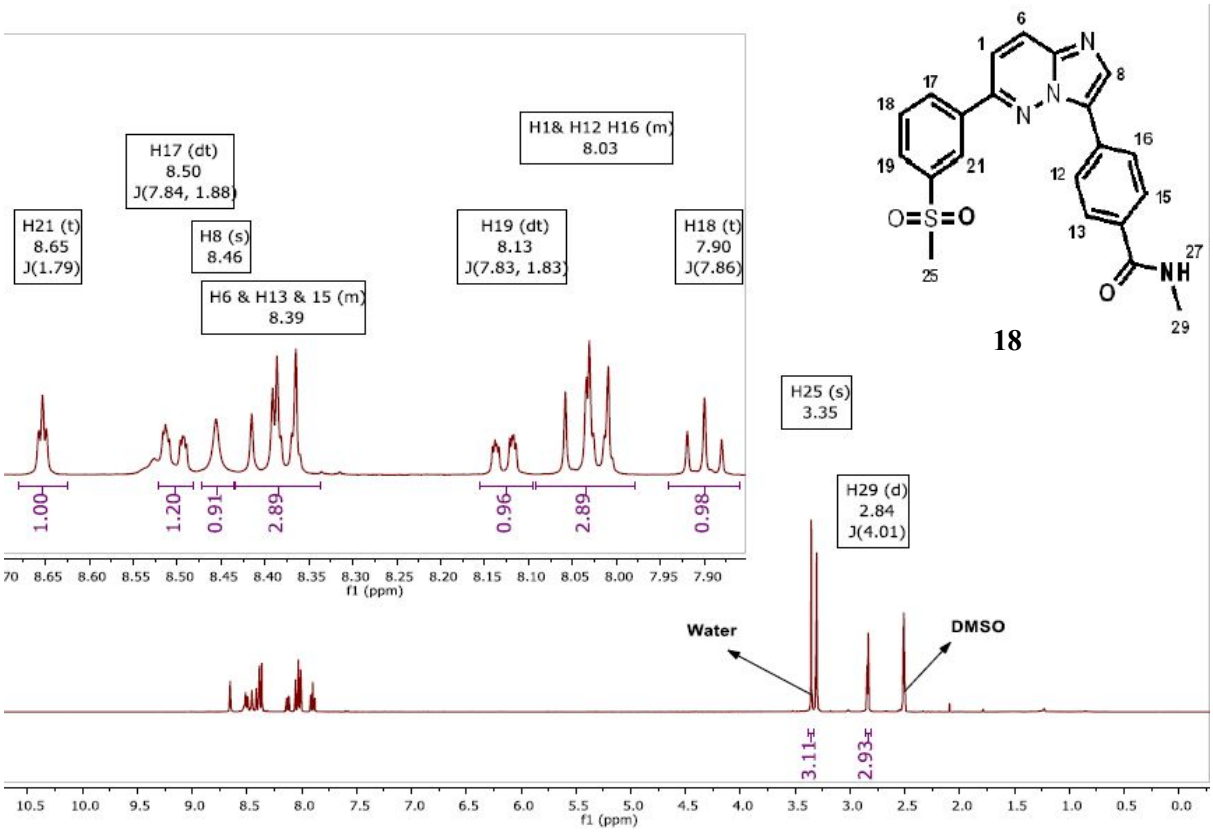
H17 (dt)
8.50
J(7.84, 1.88)
H1& H12 H16 (m)
8.03
H21 (t)
8.65
J(1.79)
H8 (s)
8.46
H19 (dt)
8.13
J(7.83, 1.83)
H18 (t)
7.90
J(7.86)
H6 & H13 & 15 (m)
8.39
18
H25 (s)
3.35
H29 (d)
2.84
J(4.01)
Water
DMSO
f1 (ppm)

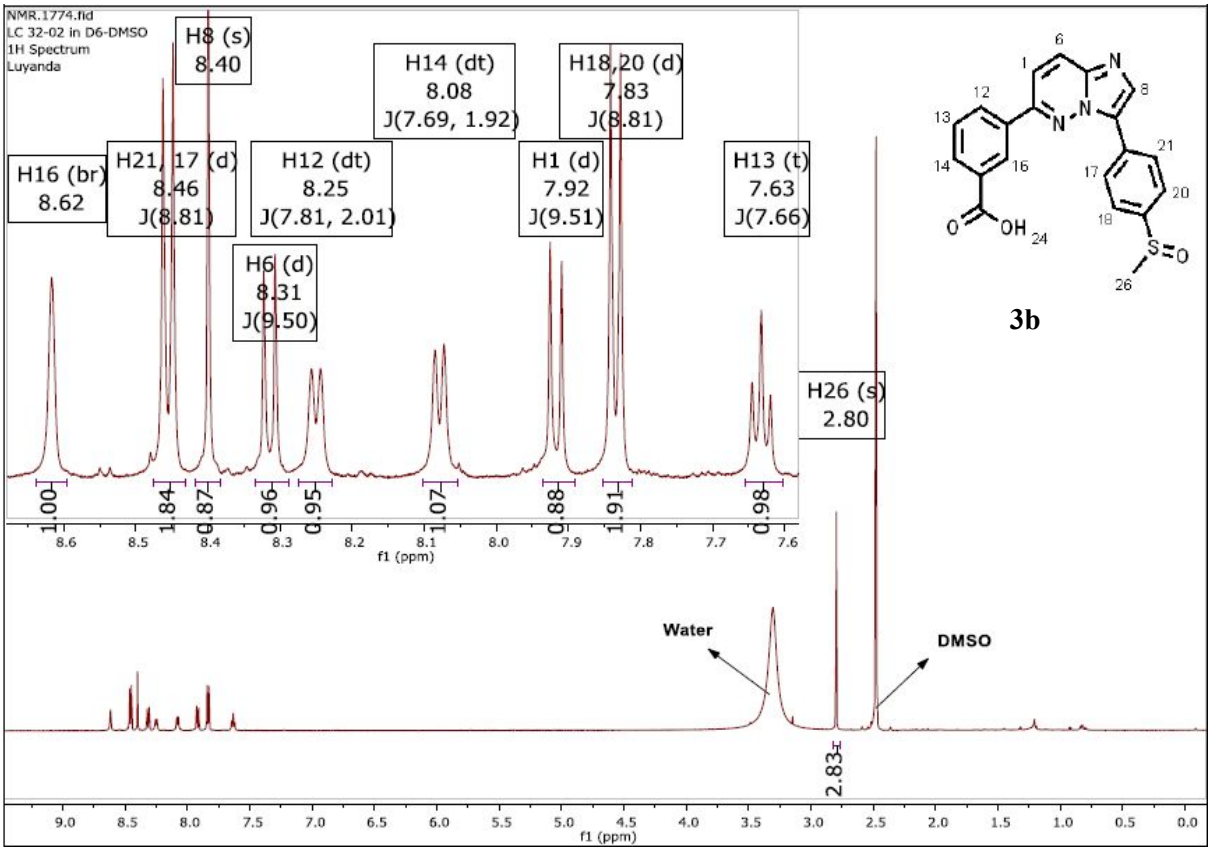
NMR.1774.fid
LC 32-02 in D6-DMSO
1H Spectrum
Luyanda
H8 (s)
8.40
H14 (dt)
8.08
J(7.69, 1.92)
H18,20 (d)
7.83
J(8.81)
H16 (br)
8.62
H21, 17 (d)
8.46
J(8.81)
H12 (dt)
8.25
J(7.81, 2.01)
H1 (d)
7.92
J(9.51)
H13 (t)
7.63
J(7.66)
H6 (d)
8.31
J(9.50)
H26 (s)
2.80
Water
DMSO
f1 (ppm)

3b

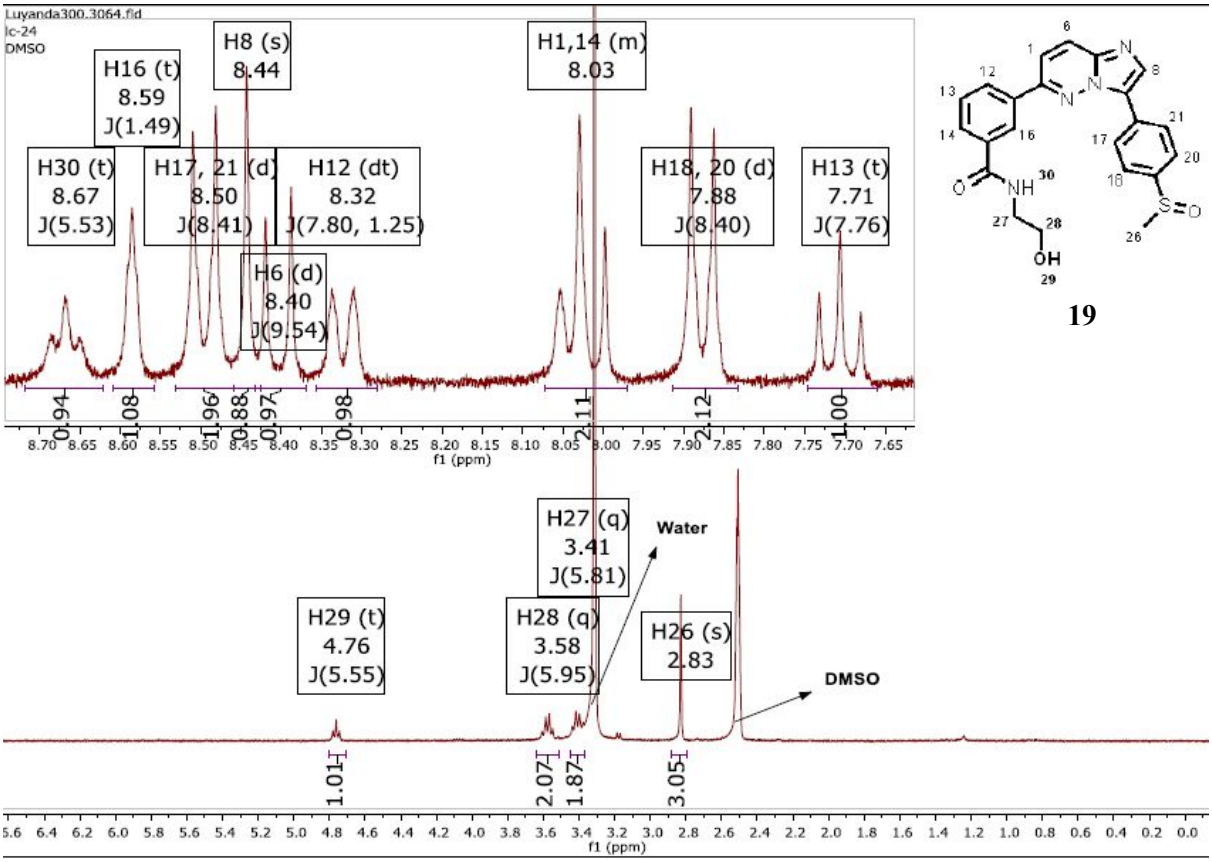
Luyanda300.3064.fid
lc-24
DMSO
H8 (s)
8.44
H1,14 (m)
8.03
H16 (t)
8.59
J(1.49)
H30 (t)
8.67
J(5.53)
H17, 21 (d)
8.50
J(8.41)
H12 (dt)
8.32
J(7.80, 1.25)
H18, 20 (d)
7.88
J(8.40)
H13 (t)
7.71
J(7.76)
H6 (d)
8.40
J(9.54)
H27 (q)
3.41
J(5.81)
Water
H29 (t)
4.76
J(5.55)
H28 (q)
3.58
J(5.95)
H26 (s)
2.83
DMSO
f1 (ppm)

19

1H NMR (400 MHz, Methanol-d4) δ 8.53 (td, J = 1.9, 0.5 Hz, 1H), 8.46 (d, J = 8.8 Hz, 2H), 8.28 – 8.23 (m, 2H), 8.18 (d, J = 9.6 Hz, 1H), 7.98 (ddd, J = 7.8, 1.8, 1.1 Hz, 1H), 7.92 – 7.86 (m, 3H), 7.66 (td, J = 7.8, 0.6 Hz, 1H), 3.00 (s, 3H), 2.90 (s, 3H).

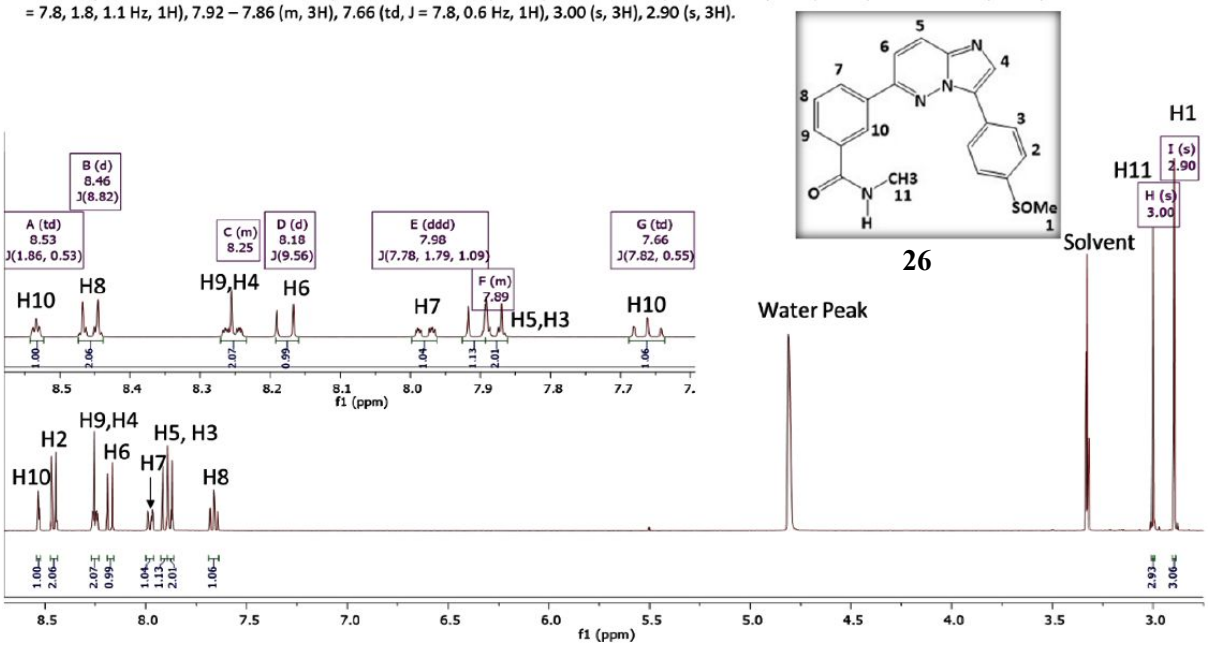

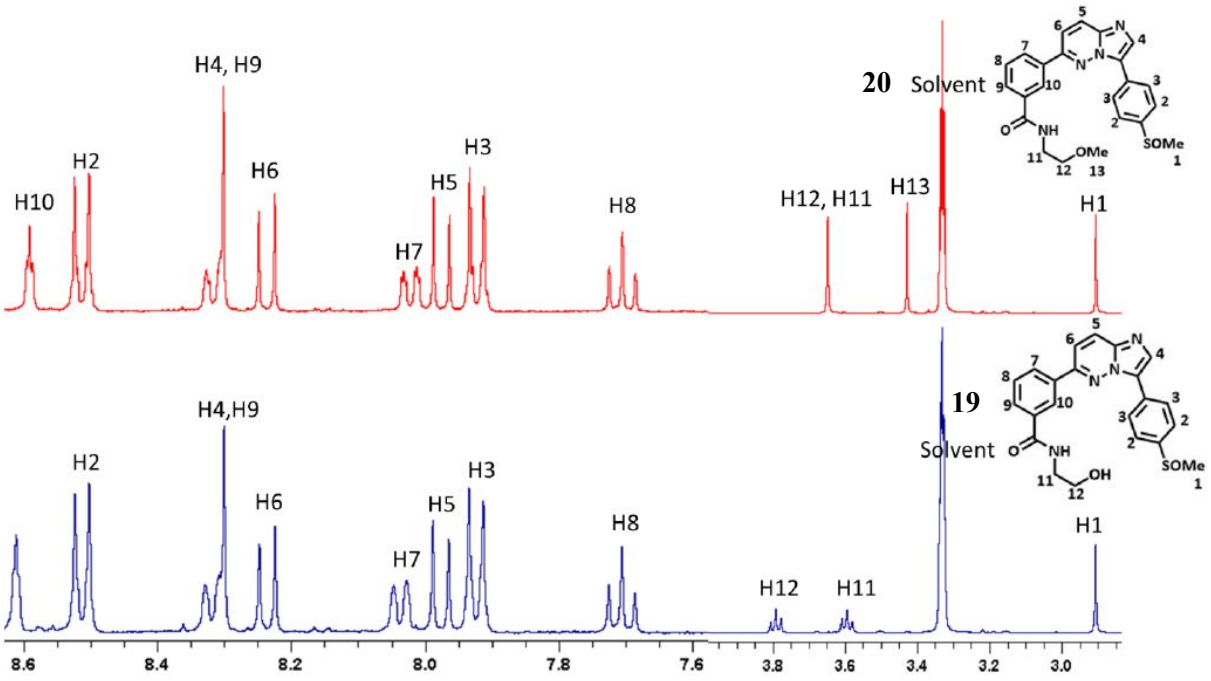

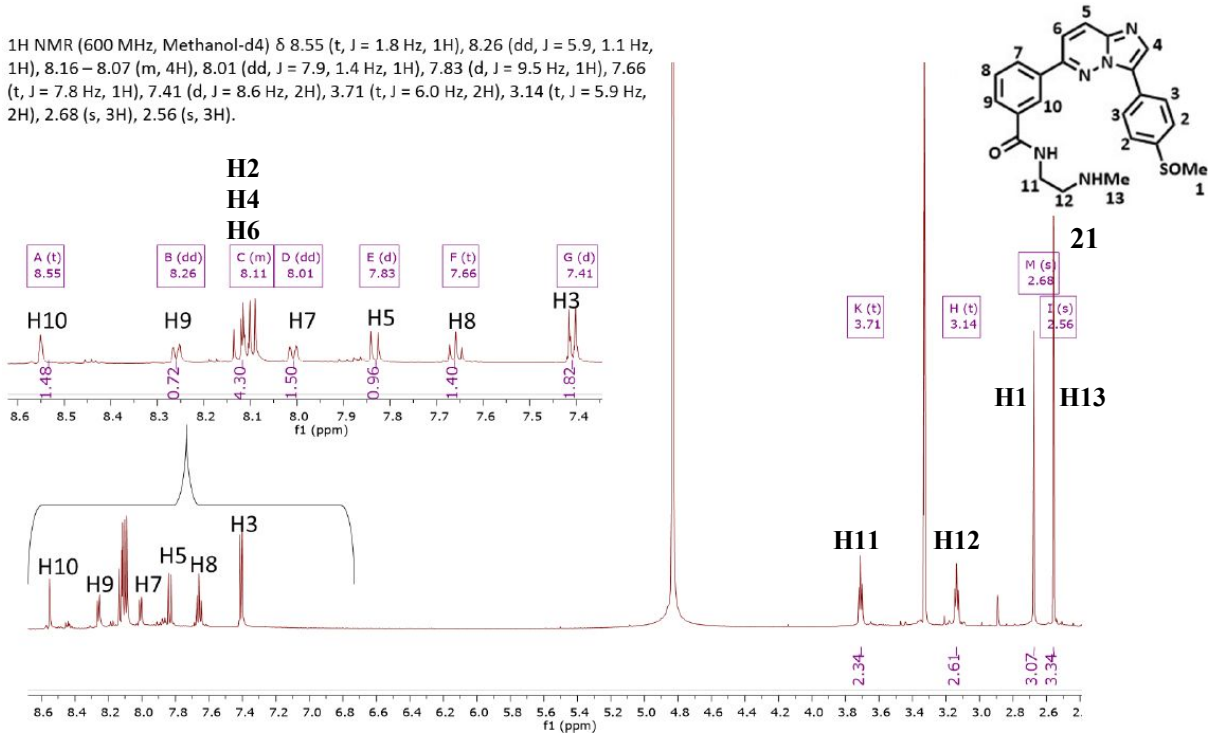

5.0 Additional References

(1) Desjardins, R. E.; Canfield, C. J.; Haynes, J. D.; Chulay, J. D. Quantitative Assessment of Antimalarial Activity in Vitro by a Semiautomated Microdilution Technique. *Antimicrobial Agents and Chemotherapy* **1979**, *16*, 710–718.

(2) Dorn, A.; Stoffel, R.; Matile, H.; Bubendorf, A.; Ridley, R. G. Malarial Haemozoin/β-Haematin Supports Haem Polymerization in the Absence of Protein. *Nature.* **1995**, *374*, 269–271.

(3) Trager, W.; Jensen, J. Human Malaria Parasites in Continuous Culture. *Science* **1976**, *193*, 673–675.

(4) Huber, W.; Koella, J. C. A Comparison of Three Methods of Estimating EC50 in Studies of Drug Resistance of Malaria Parasites. *Acta Tropica* **1993**, *55*, 257–261.

(5) Piper, R. C.; Williams, J. A.; Makler, M. T.; Gibbins, B. L.; Hinrichs, D. J.; Ries, J. M.; Bancroft, J. E. Parasite Lactate Dehydrogenase as an Assay for Plasmodium Falciparum Drug Sensitivity. *The American Journal of Tropical Medicine and Hygiene* **1993**, *48*, 739–741.

(6) Reader, J.; Botha, M.; Theron, A.; Lauterbach, S. B.; Rossouw, C.; Engelbrecht, D.; Wepener, M.; Smit, A.; Leroy, D.; Mancama, D.; Coetzer, T. L.; Birkholtz, L.-M. Nowhere to Hide: Interrogating Different Metabolic Parameters of Plasmodium Falciparum Gametocytes in a Transmission Blocking Drug Discovery Pipeline towards Malaria Elimination. *Malar J* **2015**, *14*, 213.

(7) Reader, J.; van der Watt, M. E.; Taylor, D.; Le Manach, C.; Mittal, N.; Ottilie, S.; Theron, A.; Moyo, P.; Erlank, E.; Nardini, L.; Venter, N.; Lauterbach, S.; Bezuidenhout, B.; Horatscheck, A.; van Heerden, A.; Boyle, G. A.; Calvo, D.; Mancama, D.; Coetzer, T. L.; Winzeler, E. A.; Duffy, J.; Koekemoer, L. L.; Basarab, G.; Chibale, K.; Birkholtz, L.-M. Multistage and Transmission-Blocking Targeted Antimalarials Discovered from the Open-Source MMV Pandemic Response Box. **2020** (a preprint). DOI: 10.1101/2020.06.05.133405

(8) McNamara, C. W.; Lee, M. C. S.; Lim, C. S.; Lim, S. H.; Roland, J.; Nagle, A.; Simon, O.; Yeung, B. K. S.; Chatterjee, A. K.; McCormack, S. L.; Manary, M. J.; Zeeman, A.-M.; Dechering, K. J.; Kumar, T. R. S.; Henrich, P. P.; Gagaring, K.; Ibanez, M.; Kato, N.; Kuhen, K. L.; Fischli, C.; Rottmann, M.; Plouffe, D. M.; Bursulaya, B.; Meister, S.; Rameh, L.; Trappe, J.; Haasen, D.; Timmerman, M.; Sauerwein, R. W.; Suwanarusk, R.; Russell, B.; Renia, L.; Nosten, F.; Tully, D. C.; Kocken, C. H. M.; Glynne, R. J.; Bodenreider, C.; Fidock, D. A.; Diagana, T. T.; Winzeler, E. A. Targeting Plasmodium PI(4)K to Eliminate Malaria. *Nature* **2013**, *504*, 248–253.

(9) Kato, N.; Comer, E.; Sakata-Kato, T.; Sharma, A.; Sharma, M.; Maetani, M.; Bastien, J.; Brancucci, N. M.; Bittker, J. A.; Corey, V.; Clarke, D.; Derbyshire, E. R.; Dornan, G. L.; Duffy, S.; Eckley, S.; Itoe, M. A.; Koolen, K. M. J.; Lewis, T. A.; Lui, P. S.; Lukens, A. K.; Lund, E.; March, S.; Meibalan, E.; Meier, B. C.; McPhail, J. A.; Mitasev, B.; Moss, E. L.; Sayes, M.; Van Gessel, Y.; Wawer, M. J.; Yoshinaga, T.; Zeeman, A.-M.; Avery, V. M.; Bhatia, S. N.; Burke, J. E.; Catteruccia, F.; Clardy, J. C.; Clemons, P. A.;

Dechering, K. J.; Duvall, J. R.; Foley, M. A.; Gusovsky, F.; Kocken, C. H. M.; Marti, M.; Morningstar, M. L.; Munoz, B.; Neafsey, D. E.; Sharma, A.; Winzeler, E. A.; Wirth, D. F.; Scherer, C. A.; Schreiber, S. L. Diversity-Oriented Synthesis Yields Novel Multistage Antimalarial Inhibitors. *Nature* **2016**, *538*, 344–349.

(10) Baker, D. A.; Stewart, L. B.; Large, J. M.; Bowyer, P. W.; Ansell, K. H.; Jiménez-Díaz, M. B.; El Bakkouri, M.; Birchall, K.; Dechering, K. J.; Bouloc, N. S.; Coombs, P. J.; Whalley, D.; Harding, D. J.; Smiljanic-Hurley, E.; Wheldon, M. C.; Walker, E. M.; Dessens, J. T.; Lafuente, M. J.; Sanz, L. M.; Gamo, F.-J.; Ferrer, S. B.; Hui, R.; Bousema, T.; Angulo-Barturén, I.; Merritt, A. T.; Croft, S. L.; Gutteridge, W. E.; Kettleborough, C. A.; Osborne, S. A. A Potent Series Targeting the Malarial CGMP-Dependent Protein Kinase Clears Infection and Blocks Transmission. *Nat Commun* **2017**, *8*, 430.

(11) Vanaerschot, M.; Murithi, J. M.; Pasaje, C. F. A.; Ghidelli-Disse, S.; Dwomoh, L.; Bird, M.; Spottiswoode, N.; Mittal, N.; Arendse, L. B.; Owen, E. S.; Wicht, K. J.; Siciliano, G.; Bösche, M.; Yeo, T.; Kumar, T. R. S.; Mok, S.; Carpenter, E. F.; Giddins, M. J.; Sanz, O.; Ottilie, S.; Alano, P.; Chibale, K.; Llinás, M.; Uhlemann, A.-C.; Delves, M.; Tobin, A. B.; Doerig, C.; Winzeler, E. A.; Lee, M. C. S.; Niles, J. C.; Fidock, D. A. Inhibition of Resistance-Refractory P. Falciparum Kinase PKG Delivers Prophylactic, Blood Stage, and Transmission-Blocking Antiplasmodial Activity. *Cell Chemical Biology* **2020**.

(12) Penzo, M.; de las Heras-Dueña, L.; Mata-Cantero, L.; Diaz-Hernandez, B.; Vazquez-Muñiz, M.-J.; Ghidelli-Disse, S.; Drewes, G.; Fernandez-Alvaro, E.; Baker, D. A. High-Throughput Screening of the Plasmodium Falciparum CGMP-Dependent Protein Kinase Identified a Thiazole Scaffold Which Kills Erythrocytic and Sexual Stage Parasites. *Scientific Reports* **2019**, *9*, 7005.

(13) Cabrera, D. G.; Horatscheck, A.; Wilson, C. R.; Basarab, G.; Eyermann, C. J.; Chibale, K. Plasmodial Kinase Inhibitors: License to Cure? *J. Med. Chem.* **2018**, *61*, 8061–8077.

(14) Madhavi Sastry, G.; Adzhigirey, M.; Day, T.; Annabhimoju, R.; Sherman, W. Protein and Ligand Preparation: Parameters, Protocols, and Influence on Virtual Screening Enrichments. *J Comput Aided Mol Des* **2013**, *27*, 221–234.

(15) Harder, E.; Damm, W.; Maple, J.; Wu, C.; Reboul, M.; Xiang, J. Y.; Wang, L.; Lupyan, D.; Dahlgren, M. K.; Knight, J. L.; Kaus, J. W.; Cerutti, D. S.; Krilov, G.; Jorgensen, W. L.; Abel, R.; Friesner, R. A. OPLS3: A Force Field Providing Broad Coverage of Drug-like Small Molecules and Proteins. *J. Chem. Theory Comput.* **2016**, *12*, 281–296.

(16) Friesner, R. A.; Banks, J. L.; Murphy, R. B.; Halgren, T. A.; Klicic, J. J.; Mainz, D. T.; Repasky, M. P.; Knoll, E. H.; Shelley, M.; Perry, J. K.; Shaw, D. E.; Francis, P.; Shenkin, P. S. Glide: A New Approach for Rapid, Accurate Docking and Scoring. 1. Method and Assessment of Docking Accuracy. *J. Med. Chem.* **2004**, *47*, 1739–1749.

(17) Halgren, T. A.; Murphy, R. B.; Friesner, R. A.; Beard, H. S.; Frye, L. L.; Pollard, W. T.; Banks, J. L. Glide: A New Approach for Rapid, Accurate Docking and Scoring. 2. Enrichment Factors in Database Screening. *J. Med. Chem.* **2004**, *47*, 1750–1759.

(18) Friesner, R. A.; Murphy, R. B.; Repasky, M. P.; Frye, L. L.; Greenwood, J. R.; Halgren, T. A.; Sanschagrin, P. C.; Mainz, D. T. Extra Precision Glide: Docking and Scoring Incorporating a Model of Hydrophobic Enclosure for Protein−Ligand Complexes. *J. Med. Chem.* **2006**, *49*, 6177–6196.

(19) Shelley, J. C.; Cholleti, A.; Frye, L. L.; Greenwood, J. R.; Timlin, M. R.; Uchimaya, M. Epik: A Software Program for PK a Prediction and Protonation State Generation for Drug-like Molecules. *J Comput Aided Mol Des* **2007**, *21*, 681–691.

(20) Greenwood, J. R.; Calkins, D.; Sullivan, A. P.; Shelley, J. C. Towards the Comprehensive, Rapid, and Accurate Prediction of the Favorable Tautomeric States of Drug-like Molecules in Aqueous Solution. *J Comput Aided Mol Des* **2010**, *24*, 591–604.

(21) Jacobson, M. P.; Friesner, R. A.; Xiang, Z.; Honig, B. On the Role of the Crystal Environment in Determining Protein Side-Chain Conformations. *Journal of Molecular Biology* **2002**, *320*, 597–608.

(22) Mosmann, T. Rapid Colorimetric Assay for Cellular Growth and Survival: Application to Proliferation and Cytotoxicity Assays. *Journal of Immunological Methods.* **1983**, *65*, 55–63.

(23) Hill, A. P.; Young, R. J. Getting Physical in Drug Discovery: A Contemporary Perspective on Solubility and Hydrophobicity. *Drug Discovery Today.* **2010**, *15*, 648–655.

(24) Bevan, C. D.; Lloyd, R. S. A High-Throughput Screening Method for the Determination of Aqueous Drug Solubility Using Laser Nephelometry in Microtiter Plates. *Analytical Chemistry* **2000**, *72*, 1781–1787.